A revision of *Prolimulus woodwardi* Fritsch, 1899 with comparison to other highly paedomorphic belinurids

Lorenzo Lustri[1], Lukáš Laibl[2,3] and Russell D.C. Bicknell[4]

[1] Institute of Earth Sciences, University of Lausanne, Geopolis, Lausanne, Switzerland
[2] Institute of Geology and Palaeontology, Faculty of Science, Charles University, Prague, Czech Republic
[3] Institute of Geology of the Czech Academy of Sciences, Prague, Czech Republic
[4] Palaeoscience Research Centre, School of Environmental and Rural Science, University of New England, Armidale, New South Wales, Australia

ABSTRACT

Xiphosurida is an ingroup of marine Euchelicerata often referred to as "living fossils". However, this oxymoronic term is inapplicable for Paleozoic and early Mesozoic forms, as during these periods the group experienced notable evolutionary radiations; particularly the diverse late Palaeozoic clade Belinurina. Despite the iconic nature of the group, select species in this clade have been left undescribed in the light of recent geometric morphometric and phylogenetic considerations and methodologies. To this end, we re-describe *Prolimulus woodwardi* *Fritsch, 1899* using new and type specimens to reveal more details on appendage anatomy and possible ecology. Furthermore, we present geometric morphometric and phylogenetic analyses that uncover relationships between *P. woodwardi* and other belinurids without genal spines. Both approaches highlight that a clade containing *Prolimulus* *Fritsch, 1899*, *Liomesaspis* *Raymond, 1944*, *Alanops* *Racheboeuf, Vannier & Anderson, 2002* and *Stilpnocephalus* *Selden, Simonetto & Marsiglio, 2019* may exist. While we do not erect a new group to contain these genera, we note that these genera exemplify the extreme limits of the Belinurina radiation and a peak in horseshoe crab diversity and disparity. This evidence also illustrates how changes in heterochronic timing are a key evolutionary phenomenon that can drive radiations among animals.

Submitted 27 November 2020
Accepted 30 January 2021
Published 8 March 2021

Corresponding author
Lorenzo Lustri, lorenzo.lustri@unil.ch

Academic editor
Brandon Hedrick

Additional Information and Declarations can be found on page 26

DOI **10.7717/peerj.10980**

Subjects Evolutionary Studies, Marine Biology, Paleontology, Taxonomy, Zoology
Keywords Xiphosurida, Belinuridae, Carboniferous, Heterochrony, Epibiota

INTRODUCTION

Xiphosurida, are an extant group of eucheliceratesith an extensive fossil record spanning most of the Phanerozoic (*Van Roy, Briggs & Gaines, 2015*). They are often referred to as "living fossils" (*Størmer, 1952*), considered examples of stabilomorphism (*Kin & Błażejowski, 2014*) and morphological conservatism (*Bicknell & Pates, 2020*). Such statements are mostly applicable to the late Mesozoic and Cenozoic forms (*Avise, Nelson & Sugita, 1994*; *Rudkin & Young, 2009*; *Kin & Błażejowski, 2014*; *Lamsdell & McKenzie, 2015*; *Błazejowski, Gieszcz & Tyborowski, 2016*; *Bicknell & Pates, 2019*; *Bicknell et al., 2019b*; *Bicknell & Pates, 2019*). Conversely, most Paleozoic and early Mesozoic forms record evolutionary exploration (*Bicknell, 2019*; *Bicknell, Amati & Hernández, 2019*; *Bicknell et al., 2019a*; *Bicknell,*

Naugolnykh & Brougham, 2020; *Bicknell et al., in press*; *Bicknell, Hecker & Heyng , 2021*; *Bicknell & Pates, 2020*). The evolutionary history of these earlier species illustrate morphological plasticity and exploration of different ecological niches (*Lamsdell, 2016*; *Lamsdell, 2020a*; *Bicknell et al., 2019b*). Belinurina—a clade containing Belinuridae—is a particularly diverse group known from the Carboniferous and Permian that successfully colonized freshwater environments. Belinurids have been considered at length (*Størmer, 1952*; *Eldredge, 1974*; *Anderson & Selden, 1997*; *Haug et al., 2012*; *Haug & Haug, 2020*) and the presence of hypertrophied genal spines or complete loss of genal spines characterizes the group. Furthermore, phylogenetic analyses illustrated that Belinurina was a monophyletic superfamily traditionally thought to contain *Alanops* (*Racheboeuf, Vannier & Anderson, 2002*), *Anacontium* (*Raymond, 1944*), *Belinurus* (*Pictet, 1846*), *Euproops* (*Meek & Worthen, 1865*), *Liomesaspis* (*Raymond, 1944*), and *Prolimulus* (*Fritsch, 1899*). Despite the interest in belinurids, an array of species described in the early 20th century require revision (see *Lamsdell & McKenzie, 2015*; *Bicknell et al., 2019a*: *Bicknell, Lustri & Brougham, 2019*; *Bicknell & Pates, 2020*; *Bicknell & Smith, in press* for revisions of similar historical material). Expanding on the recent pulse in the revision of such historically important species, we reevaluate *Prolimulus woodwardi Fritsch, 1899*. We present a phylogenetic analysis including *P. woodwardi* and the morphologically comparable *Stilpnocephalus pontebbanus Selden, Simonetto & Marsiglio, 2019*, as well as a geometric morphometric analysis of species within Belinurina. These analyses highlight the extreme morphologies exhibited by *Prolimulus* and its kin, suggesting the requirement for a clade to contain these species.

GEOLOGIC AND STRATIGRAPHIC CONTEXT

Upper Paleozoic continental strata in central and western Bohemia are formally subdivided into the Plzeň, Manětín, Žihle, Radnice, Kladno-Rakovník, and Mšeno-Roudnice basins (*Pešek, 1994*; *Opluštil et al., 2013*; *Pešek, Sivek & Sivek, 2016*; Fig. 1A). Sedimentary successions within these basins comprise of four formations—the Kladno Formation (composed of older Radnice and younger Nýřany members), that unconformably overlies the basement rocks; followed by the Týnec Formation, Slaný Formation, and terminated by the Líně Formation (*Pešek, 1994*; *Opluštil et al., 2013*; Fig. 1B).

The Nýřany Member of the Kladno Formation is composed of cyclically arranged, predominantly coarse- and medium-grained sediments of fluvial origin (*Pešek, 1994*; *Opluštil, Martínek & Tasáryová, 2005*). Fine-grained sediments of floodplain, palustrine, and lacustrine origin are also present (*Opluštil, Martínek & Tasáryová, 2005*). These cycles are usually terminated by thin coal seams (*Pešek, 1994*; *Opluštil, Martínek & Tasáryová, 2005*). From a palaeoenvironmental perspective, the Nýřany Member was deposited in a large alluvial plain with a braided river system with locally developed lakes, wetlands, and peat swamps (*Opluštil, Martínek & Tasáryová, 2005*), located in a nearly equatorial latitude (*Krs, Krsová & Pruner, 1995*). Recent U-Pb dating estimated that the Nýřany Member is between 308.3–305.9 ± 0.1 Ma, spanning the late Moscovian to early Kasimovian (*Opluštil et al., 2016*; Fig. 1B).

In the Plzeň Basin, the lower parts of the Nýřany Member contain the locally developed Main Nýřany Coal with intercalated beds of lacustrine sapropelic coal

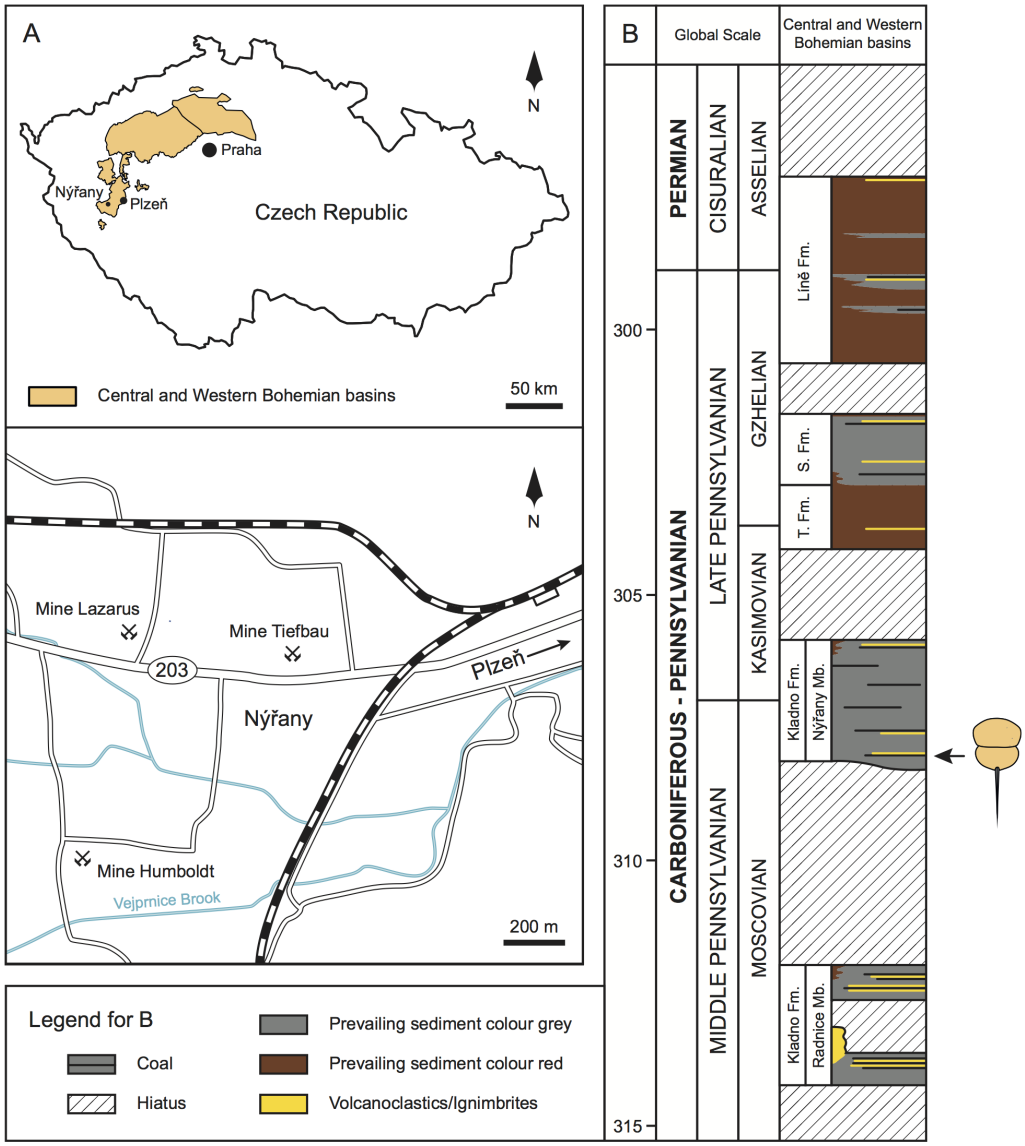

Figure 1 **Geologic and stratigraphic context of the studied material.** (A) Geographic location of the central and western Bohemian basins and location of the main historical mines in the Nýřany area. The studied material was collected from the Main Nýřany Coal, Humboldt Mine. (B) Chronostratigraphic position of the lithostratigraphic units of central and western Bohemian basins (modified from *Opluštil et al., 2016*). Arrow indicates the stratigraphic location of the studied material. Abbreviations: Fm., Formation; Mb., Member; S. Fm., Slaný Formation; T. Fm., Týnec Formation.

Full-size DOI: 10.7717/peerj.10980/fig-1

(*Fritsch, 1883*; *Purkyně, 1899*; *Pešek, 1994*; *Štamberg & Zajíc, 2008*). This sapropelic coal yielded diverse and exceptionally well-preserved fauna. Most of sapropelic coal fossils originated from the Humboldt Mine in Nýřany (near Plzeň, Fig. 1A) and represent various euarthropods (including *Prolimulus woodwardi*), acanthodians, chondrichthyans, dipnoans, actinopterygians, and early diverging tetrapods (*Fritsch, 1883*; *Fritsch, 1902*; *Štamberg & Zajíc, 2008*). After closure of the Nýřany and Třemošná coalfields, the

sapropelic coal was unavailable for sampling, until a recent excavation (*Bures & Tichavek, 2012*).

MATERIAL AND METHODS

Systematic framework

We follow the systematic taxonomy of *Lamsdell (2013)*, *Lamsdell (2016)*, *Lamsdell (2020a)*, *Bicknell, Lustri & Brougham (2019)*, and *Bicknell & Pates (2020)* and anatomical terms presented in *Selden & Siveter (1987)*, *Haug & Rötzer (2018b)*, and *Selden, Simonetto & Marsiglio (2019)*.

Specimen photography

Museums where *Prolimulus woodwardi* specimens are housed were contacted and photographs of specimens were either requested from the collection managers or made by the authors, or colleagues. Most specimens were photographed with SLR cameras under normal light. Select specimens were submerged in alcohol prior to photography to enhance contrast; however, this could not be conducted for all specimens due to collection constraints.

Phylogenetic analyses

The phylogenetic analysis was conducted to determine where *Prolimulus woodwardi* and the morphologically comparable *Stilpnocephalus pontebbanus* are located in tree space. These species were coded into the *Bicknell, Lustri & Brougham (2019)* matrix, derived from *Lamsdell (2016)*. The analysis was performed under equally weighted parsimony in TNT 1.5 (*Goloboff & Catalano, 2016*) following *Bicknell, Lustri & Brougham (2019)* and *Lamsdell (2016)*. Further, implied and equal weighted produced highly comparable trees. Five replications of a "New Technology" tree search was run using random sectorial searches, 1,000 iterations of the parsimony ratchet, 50 cycles of drifting and 5 rounds of tree fusing, holding a maximum of 10 trees per replication (Supplementary Information 1). All multistate characters were unordered (*Lamsdell, 2016*; *Bicknell, Lustri & Brougham, 2019*).

Geometric morphometric methods

Following *Bicknell et al. (2019)*, a morphometric dataset of landmarks and semilandmarks from 91 specimens across 19 species was collected to explore Belinurina morphospace. Landmarking and semilandmarking was conducted using the Thin-Plate Spline (TPS) suite (http://life.bio.sunysb.edu/morph/index.html). The TPS file was constructed using tpsUtil64 (v.1.7). The TPS file was imported into tpsDig2 (v.2.26), which was used to place four landmarks across the prosoma and thoracetron and 40 semi-landmarks along the right prosomal shield (Fig. 2; Table 1). Semilandmarks were placed in a clockwise direction along the most anterior section of the prosomal shield, coinciding with the first landmark, ending at the third landmark: the most lateral prosomal-thoracetronic articulation point. Points were digitised as *xy* coordinates. When the right side was poorly preserved, the left side was used, and these data were mirrored. These data populated the TPS file (Supplementary Information 2). TPS file was imported into R. The 'geomorph' package

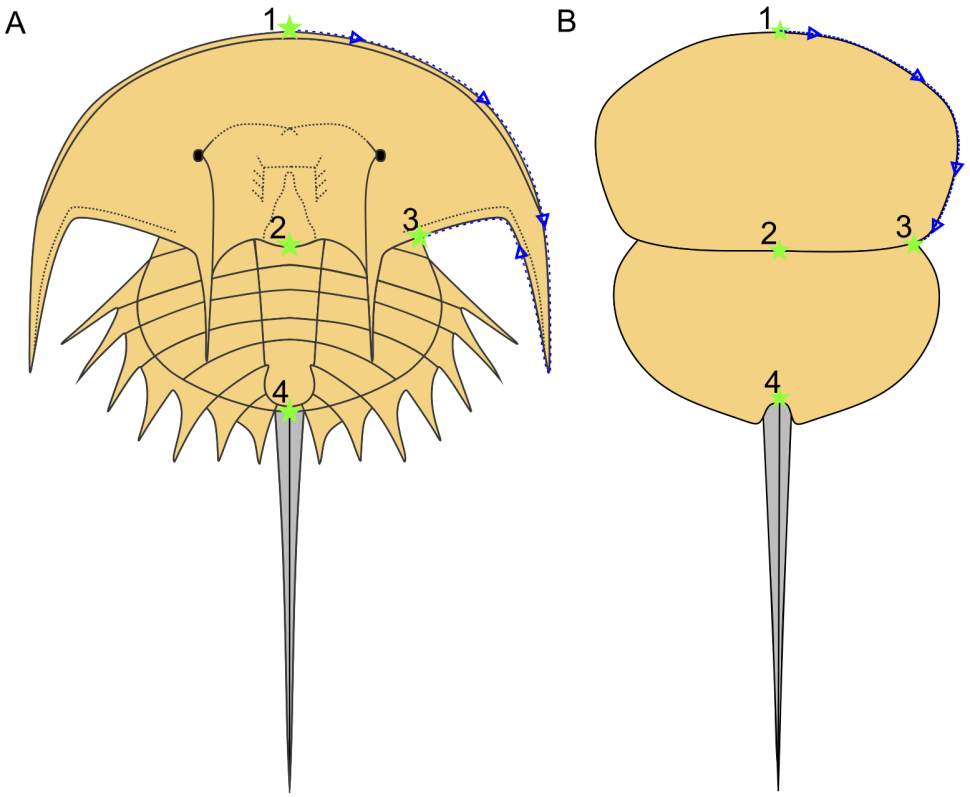

Figure 2 Approximate semilandmark trajectory (blue arrows and dotted line) and the landmarks used here. (A) Reconstruction of *Euproops danae* showing approximate landmark and semilandmark placement. (B) Reconstruction of *Prolimulus woodwardi* showing approximate landmark and semilandmark placement. Landmarks are described in Table 1.

Full-size DOI: 10.7717/peerj.10980/fig-2

(*Adams & Otárola-Castillo, 2013*) was used to conduct a Procrustes Superimposition and Principal Components Analysis (PCA) of the data (Data S3). Only the first two Principal Components (PCs) were considered as they explained 87% of the variation in the data. The examined species were representatives of *Alanops*, *Belinurus, Euproops, Liomesaspis,* and *Prolimulus*. We were unable to include *Anacontium* and *Stilpnocephalus* as opisthosomal sections are not known from these genera. We had initially used generic assignment of *Bicknell & Pates (2020)* for this analysis. However, during the course of peer review, *Lamsdell (2020b)* presented a revision of Xiphosurida and proposed that Belinurina consisted of 14 genera. To compare, contrast, and explore the distribution of these newly erected groups with the more conservative perspective of *Bicknell & Pates (2020)*, we presented the distribution of genera suggested in *Bicknell & Pates (2020)* and *Lamsdell (2020b)*.

Table 1 Description of landmarks. Landmarks used for the geometric morphometric analysis depicted in Fig. 2.

Landmark number	Description of landmark
Landmark 1	Anterior-most prosomal point along organismal sagittal line
Landmark 2	Distal-most prosomal point along organismal sagittal line
Landmark 3	Lateral-most section of prosomal-thoracetron articulation
Landmark 4	Thoracetron-telson articulation

SYSTEMATIC PALAEONTOLOGY

Euchelicerata sensu *Weygoldt & Paulus, 1979*

Xiphosurida sensu *Latreille, 1802*

Belinurina sensu *Zittel & Eastman, 1913*

Belinuridae sensu *Zittel & Eastman, 1913*

Prolimulus *Fritsch, 1899*

Amended diagnosis: Belinurid with a round prosoma that is slightly wider than long. No eyes, cardiac lobe, or ophthalmic ridges are present. Thoracetron is completely fused, without traces of segmentation, often showing a thoracetronic doublure. Thoracetron-telson articulation is 'U'-shaped. Telson is keeled.

Prolimulus woodwardi (*Fritsch, 1899*)

Figs. 3–12

1899 *Prolimulus woodwardi* Fritsch, p. 58

1902 *Prolimulus woodwardi* Fritsch, Fritsch p. 64

1938 *Prolimulus* Fritsch, *Eller* (*1938*, p. 153)

1944 *Prolimulus woodwardi* Fritsch, Raymond, p. 503

1948 *Prolimulus woodwardi* Fritsch, *Branson* (*1948*, p. 991)

1952 *Prolimulus* Fritsch, Størmer, p. 636

1955 *Prolimulus woodwardi* Fritsch, Prantl & Přibyl, pl. 2

1966 *Prolimulus* Fritsch, *Strauch* (*1966*, p. 271)

1975 *Prolimulus* Fritsch, *Bergström* (*1975*, p. 303)

1984 *Prolimulus woodwardi* Fritsch, *Fisher* (*1984*, fig. 2)

1990 *Prolimulus* Fritsch, *Beall & Labandeira* (*1990*, fig. 1)

1994 *Prolimulus* Fritsch, *Rosa et al.* (*1994*, fig. 8B)

1997 *Prolimulus woodwardi* Fritsch, *Krawczyński, Filipiak & Gwoździewicz* (*1997*, p. 1271)

2005 ?*Prolimulus* Fritsch, *Crônier & Courville* (*2005*, p. 128)

2016 *Prolimulus* Fritsch, Lamsdell, p. 188

2019 *Prolimulus* Fritsch, Selden et al., p. 335

2019 *Prolimulus* Fritsch, Bicknell & Pates, p. 1

2020 *Prolimulus woodwardi* Fritsch, Bicknell & Pates, figs. 21D–21F

2020b *Prolimulus woodwardi* Fritsch, Lamsdell, p. 17

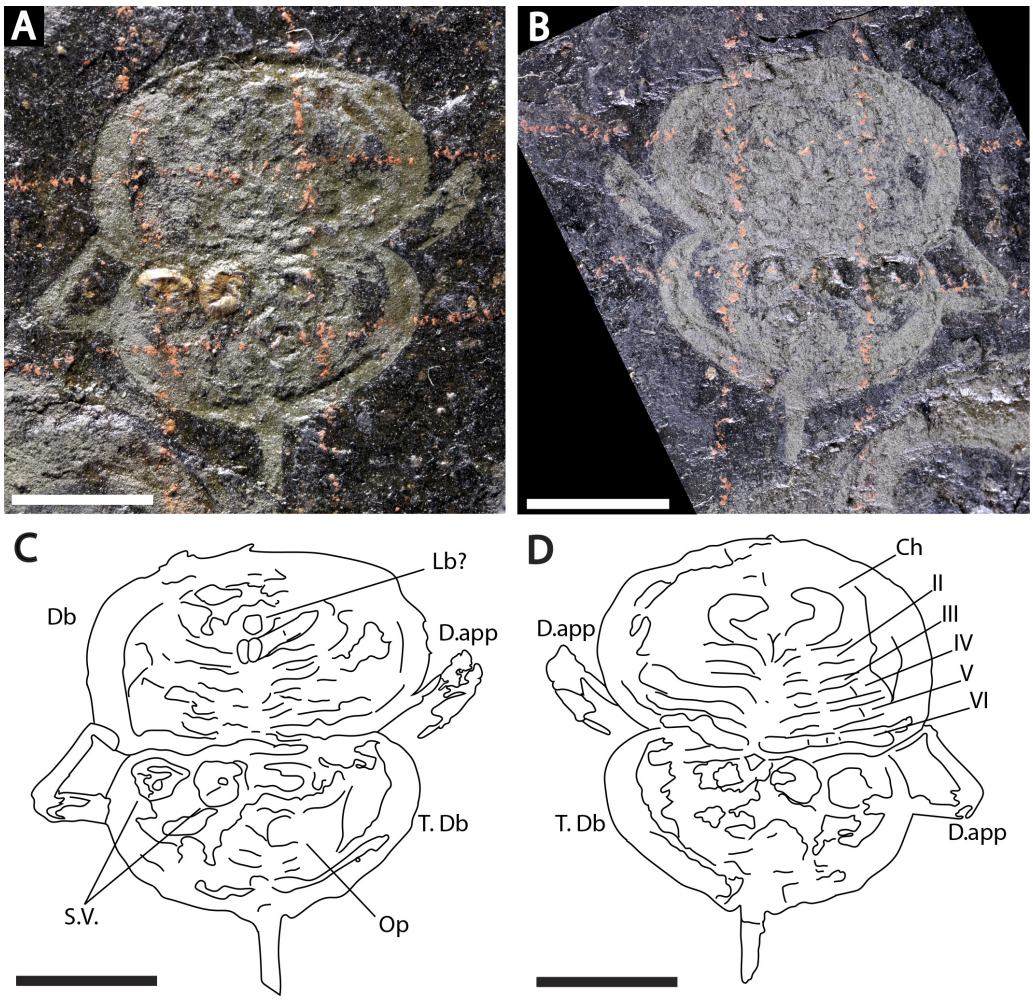

Figure 3 Holotype of *Prolimulus woodwardi* illustrating the general anatomy of the appendages. (A, C) NM Me 1031; part. (A) Complete specimen. (C) Interpretative drawing. (B, D) NM Me 1032; counterpart. (B) Complete specimen. (D) Interpretative drawing. Abbreviations: Ch: chelicera, D.app: disarticulated appendage, Db: prosomal doublure, II—VI: prosomal leg numbers, Lb: labium, Op: opercula, S.V.: *Spiroglyphus vorax*, T.Db: thoracetronic doublure. Scale bars: 10 mm. Image credit: Russell Bicknell.
Full-size DOI: 10.7717/peerj.10980/fig-3

Holotype: NM M Me 1031; NM M Me 1032
Syntype: NHMUK PI In 18588
Referred material: MB.A 1989; MCZ 109537; NM Me 39; NM Me 108; NM Me 109; NM Me 138; NM Me 139; NM Me 140; NM Me 141; NM Me 142; NM Me 143; NM Me 144; NM Me 145; NM Me 146; NM M 1038; NM M 1045; NHMUK PI I 3395.
Locality, horizon, and age: Nýřany (Humboldt Mine, active between 1865 –1902), Plzeň Basin; Main Nýřany Coal, Nýřany Member of the Kladno Formation; ~307–308 Ma, late Moscovian, Pennsylvanian.
Descriptions: NM M 1031 and NM M 1032 (Fig. 3) are part and counterpart originally described and figured by *Fritsch (1899)*, *Fritsch (1902)* and revised in *Prantl & Pribyl (1955)*. They consist of an articulated prosoma, thoracetron, and telson, preserved as

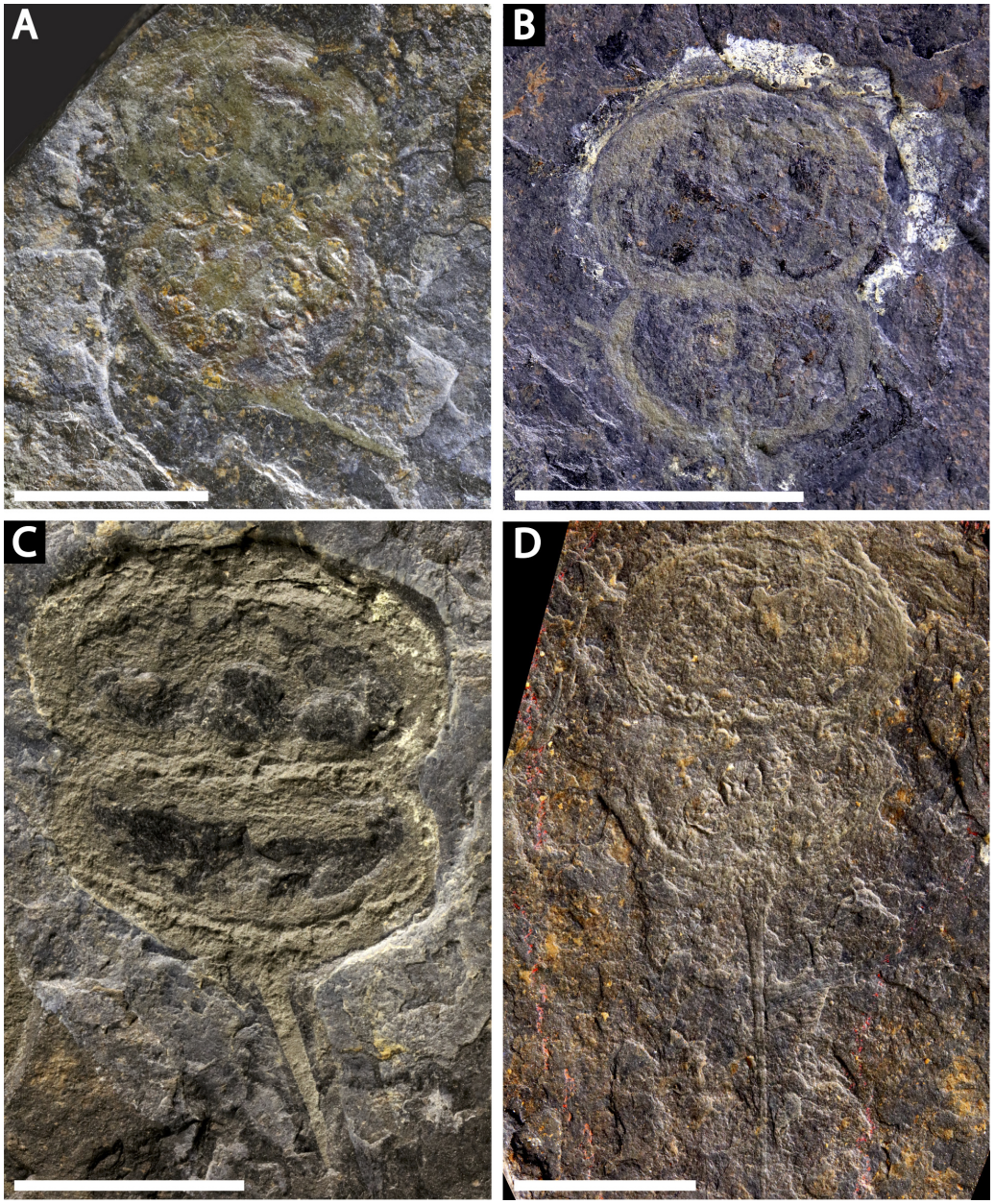

Figure 4 Four specimens of *Prolimulus woodwardi* from the National Museum of Prague Paleozoic Invertebrate collection. (A) NM Me 146. (B) NM Me 39. (C) NM Me 142. (D) NM Me 145. Scale bars: 10 mm. Image credit: Russell Bicknell.

Full-size DOI: 10.7717/peerj.10980/fig-4

flattened impressions in ventral view. Prosoma is round, slightly wider than long: 20 mm wide and 11.9 mm long. The prosomal doublure is preserved and has a maximum width of 1.9 mm. No genal spines, lateral compound eyes, cardiac lobe, or ophthalmic ridges noted. Possible traces of a labium are preserved in NM Me 1031 (Figs. 3A, 3C). Appendages are preserved and mainly visible on NM Me 1032. Chelicera are present, but chelate podomeres are not preserved (Figs. 3B, 3D). Proximal sections of walking legs are

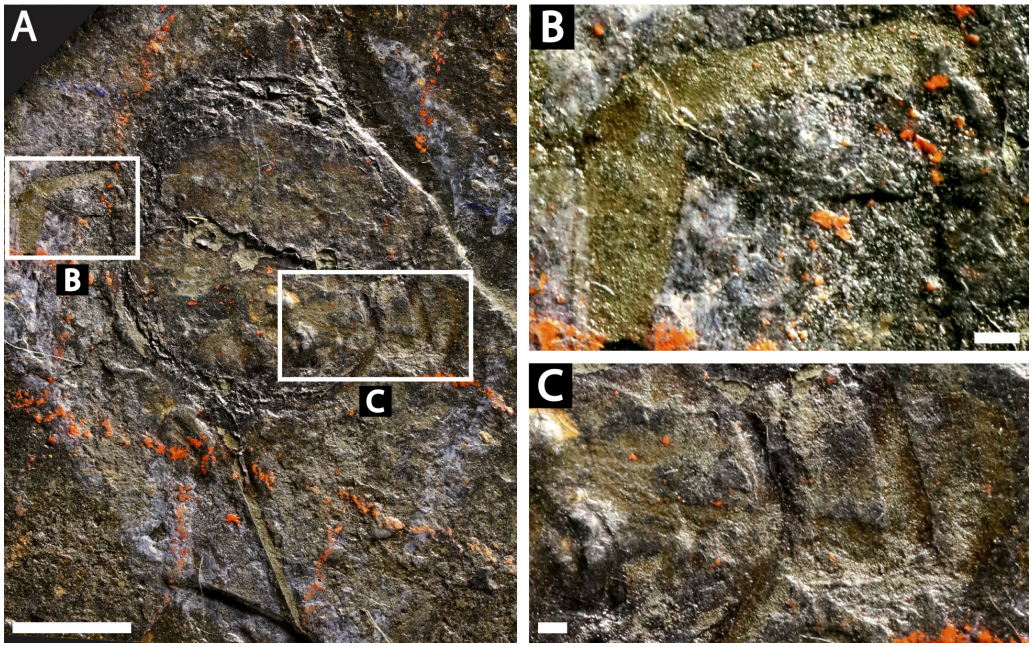

Figure 5 ***Prolimulus woodwardi*** **specimen showing detailed appendicular features.** (A, B, C) NM Me 1038. (A) Complete specimen. (B) Close up of left appendages. (C) Close up of right appendages. Scale bars: A: 10 mm, B, C: 1 mm. Image credit: Russell Bicknell.

Full-size DOI: 10.7717/peerj.10980/fig-5

preserved as slight imprints. Furthermore, podomeres of the sixth appendages are noted (Fig. 3). Third and fourth podomeres of two disarticulated appendages preserved outside prosoma. Thoracetron lacks tergal expression, is round and slightly smaller than prosoma: 18.5 mm wide and 10 mm long. No lateral spines noted. A prominent margin—likely thoracetronic doublure—preserved, is wide 2.1 mm (Fig. 3). Poorly preserved opercula are present on posterocentral thoracetron (Figs. 3A, 3C). Telson articulates with thoracetron along on posterior thoracetron margin. Telson 4.7 mm long and fragmentally preserved. Four *Spiroglyphus vorax Fritsch, 1895* specimens are attached to thoracetron.

NM Me 146 (Fig. 4A): Articulated prosoma, thoracetron and partial telson, preserved as flattened impression in ventral view. Prosoma round, slightly wider than long: 11.5 mm wide and 8.5 mm long. No prosomal doublure, genal spines, lateral compound eyes, cardiac lobe, appendages, or ophthalmic ridges noted. Thoracetron lacks tergal expression, is round, and slightly smaller than prosoma: 10.9 mm wide and 7 mm long. No lateral spines are noted. Thoracetron-telson articulation unclear, but occurs on posterior thoracetron margin. Telson partly preserved and 8.2 mm long. Two specimens of *Spiroglyphus vorax* attached to prosoma, three to prosoma-thoracetron border, and ten to thoracetron.

NM Me 39 (Fig. 4B): Articulated prosoma and thoracetron, preserved as a flattened impression in ventral view. Prosoma round, slightly wider than long: 10.5 mm wide and 7.5 mm long with a pronounced prosomal doublure. No genal spines, lateral compound eyes, cardiac lobe, appendages, or ophthalmic ridges noted. Thoracetron lacks tergal

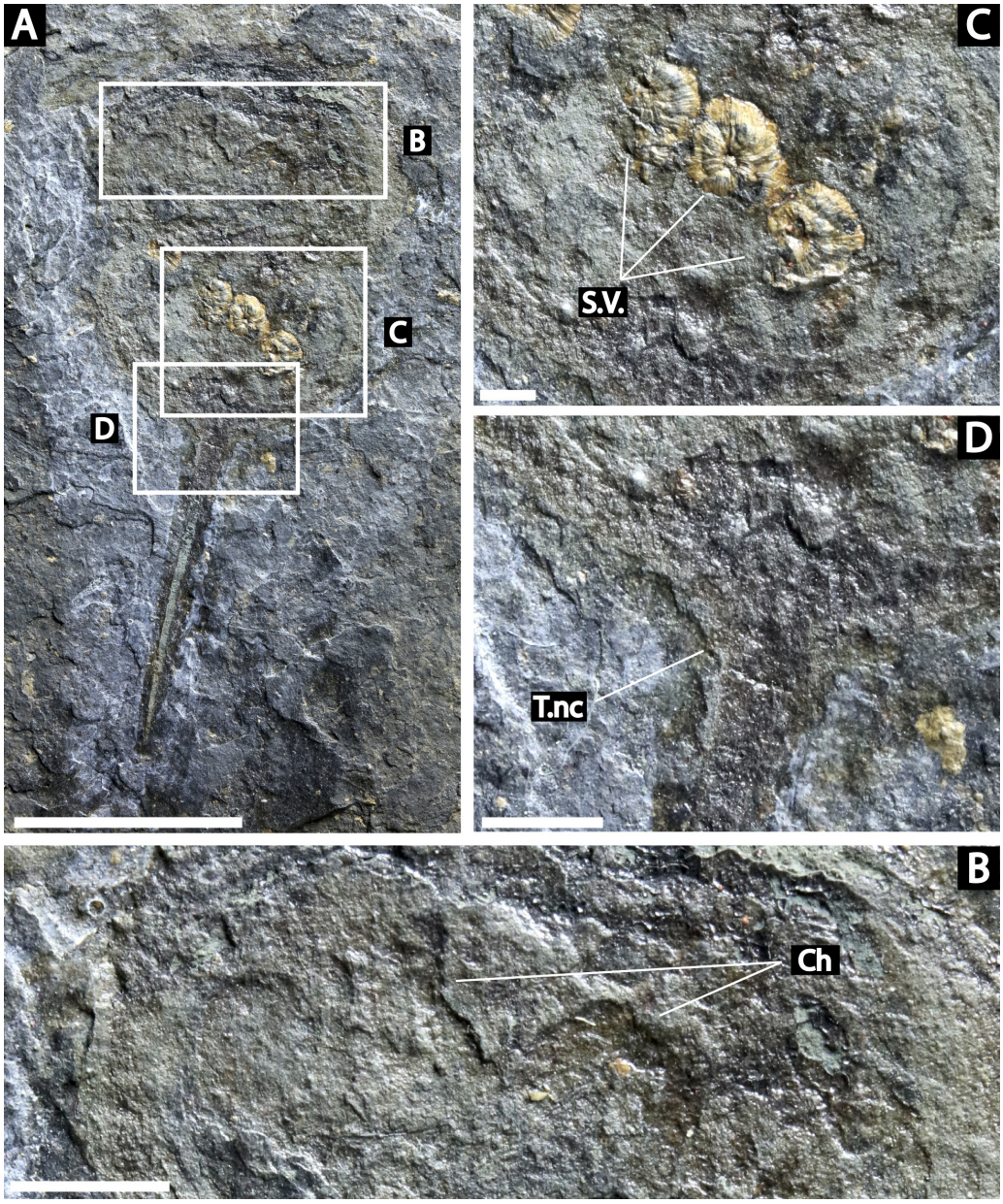

Figure 6 ***Prolimulus woodwardi*** **specimen illustrating epibionts and thoracetron-telson articulation.** (A, B, C) NM M 1045. (A) Complete specimen. (B) Close up on *Spiroglyphus vorax*. (C) Close up on telson notch. Abbreviations: Ch: chelicera, S.V.: *Spiroglyphus vorax*, T.nc: telson notch. Scale bars: A 10 mm; B 2 mm; C, D 1 mm. Image credit: Russell Bicknell.

Full-size DOI: 10.7717/peerj.10980/fig-6

expression, is round, and slightly smaller than the prosoma; 9.3 mm wide and 5.6 mm long. No lateral spines noted.

NM Me 142 (Fig. 4C): Articulated prosoma, thoracetron, and partial telson, preserved as a mostly flattened impression in ventral view. Limited relief noted in posterior prosoma, prosoma-thoracetron articulation, and anterior thoracetron. Prosoma round, slightly wider

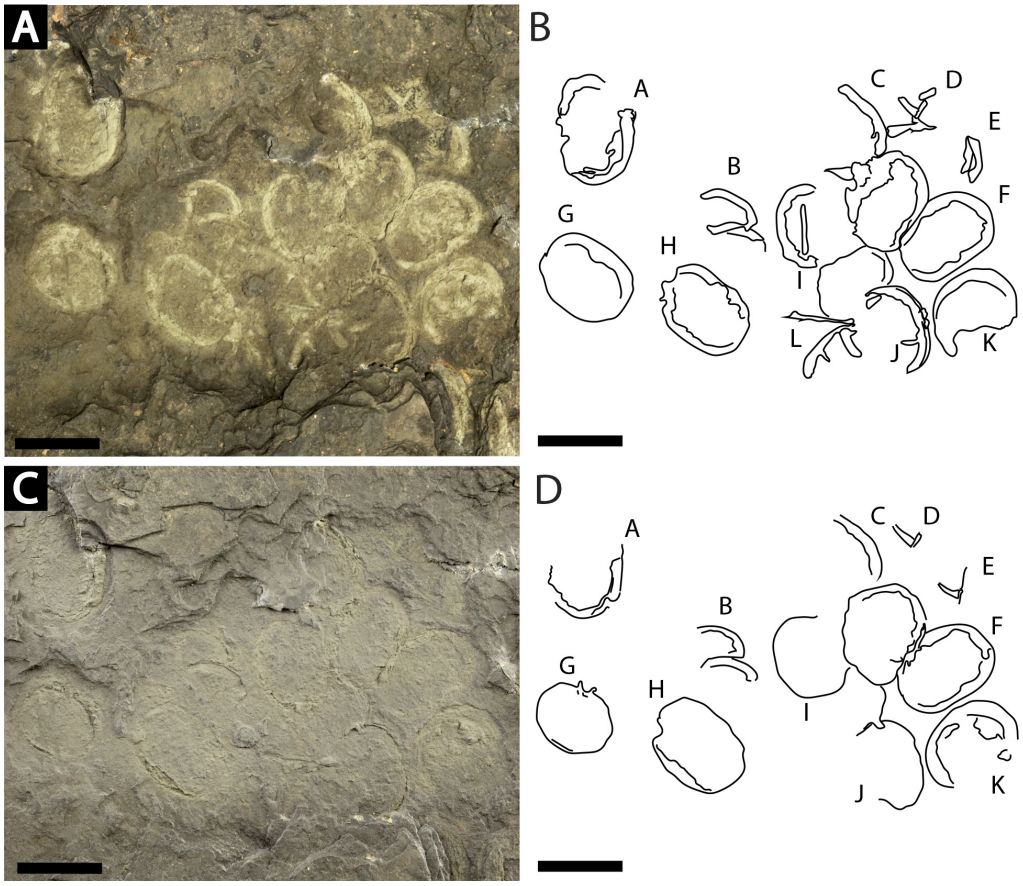

Figure 7 Slab of twelve *Prolimulus woodwardi* individuals recording possible gregarious behavior. NM Me 108. (A) Specimen photographed submerged in alcohol. (B) Interpretative drawing of (A). (C) Specimen photographed under natural light. (D) Interpretative drawing of (D). A—L indicate individual specimen designation. Scale bars: 10 mm. Image credit: Russell Bicknell.

Full-size DOI: 10.7717/peerj.10980/fig-7

than long: 12.6 mm wide and 6.8 mm long, with a pronounced prosomal doublure. No genal spines, lateral compound eyes, cardiac lobe, or ophthalmic ridges noted. Chelicera, the left set of chelate podomeres, and the proximal sections of walking legs preserved. Thoracetron lacks tergal expression, is round, and slightly larger than prosoma: 11.5 mm wide and 5.9 mm long. Pronounced thoracetronic doublure noted, 1.7 mm wide. No lateral spines noted. Thoracetron-telson articulation unclear, but occurs on posterior thoracetron margin. Telson partly preserved, 6.7 mm long.

NM Me 145 (Fig. 4D): Articulated prosoma, thoracetron, and telson, preserved as flattened impression in ventral view. Prosoma round, slightly wider than long: 13.3 mm wide and 8 mm long. No prosomal doublure, genal spines, lateral compound eyes, cardiac lobe, or ophthalmic ridges noted. No appendages are preserved. Thoracetron lacks tergal expression, is round, and slightly smaller than prosoma: 11.8 mm wide and 8.2 mm long. No lateral spines noted. Telson articulates with posterior thoracetron margin. Telson completely preserved and 15 mm long. Five *Spiroglyphus vorax* specimens attached to thoracetron.

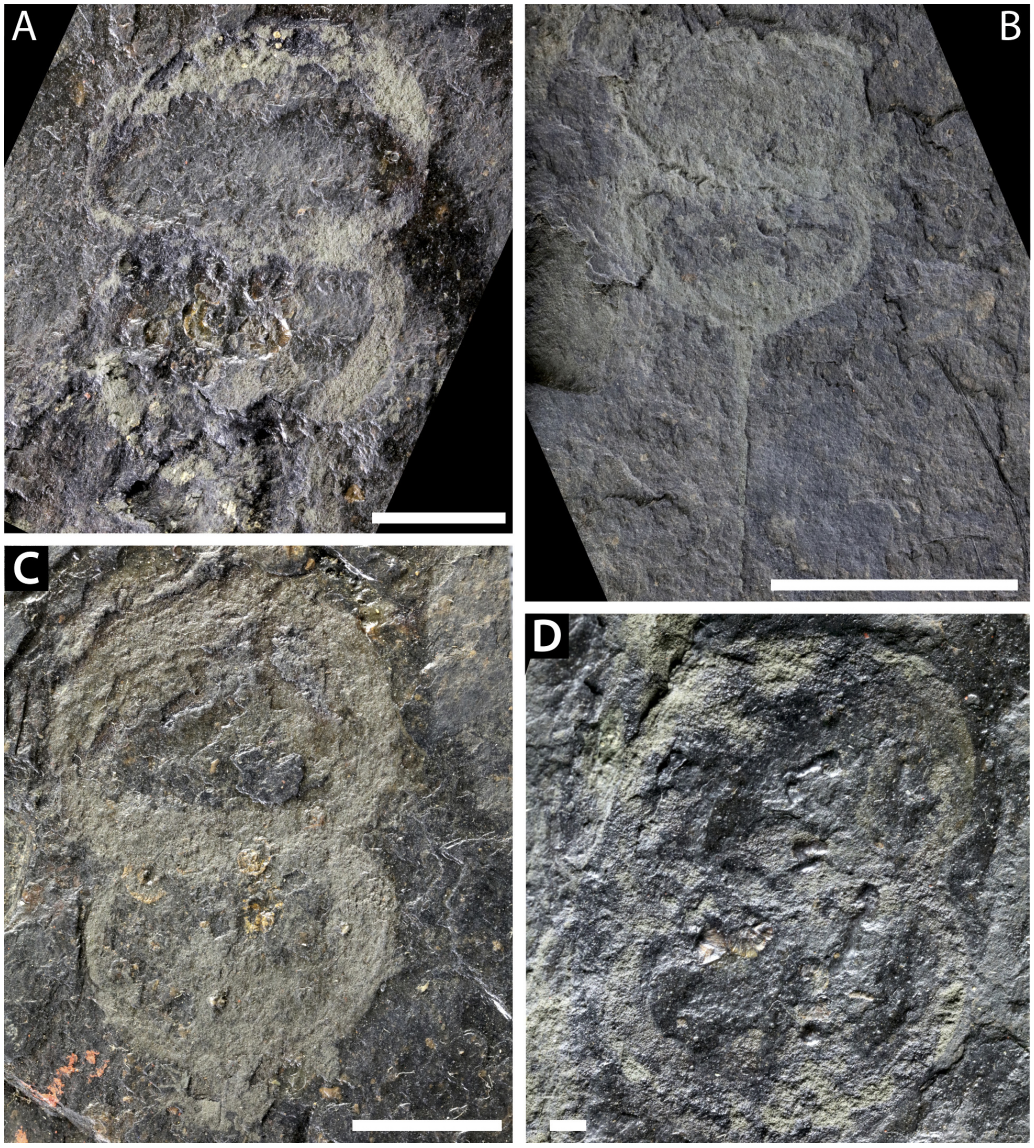

Figure 8 Further *Prolimulus woodwardi* specimens from the National Museum of Prague Paleozoic Invertebrate collection. (A) NM Me 141. (B) NM Me 109. (C) NM Me 139. (D) NM Me 143. Scale bars: A, B, C 10 mm; D 1 mm. Image credit: Russell Bicknell.

Full-size DOI: 10.7717/peerj.10980/fig-8

NM M 1038 (Fig. 5): Articulated prosoma, thoracetron, and partial telson, preserved as a flattened impression in ventral view. Prosoma round, slightly wider than long: 19 mm wide and 10.8 mm long. No prosomal doublure, genal spines, lateral compound eyes, cardiac lobe, or ophthalmic ridges noted. One disarticulated appendage preserved on left prosomal side (Fig. 5B). Thoracetron lacks tergal expression, is round, and slightly smaller than the prosoma: 17.5 mm wide and 10.3 mm long. No lateral spines noted. Thoracetron-telson articulation unclear, but occurs on posterior thoracetron margin. Telson partly preserved and 17.1 mm long. One *Spiroglyphus vorax* specimen attached to thoracetron.

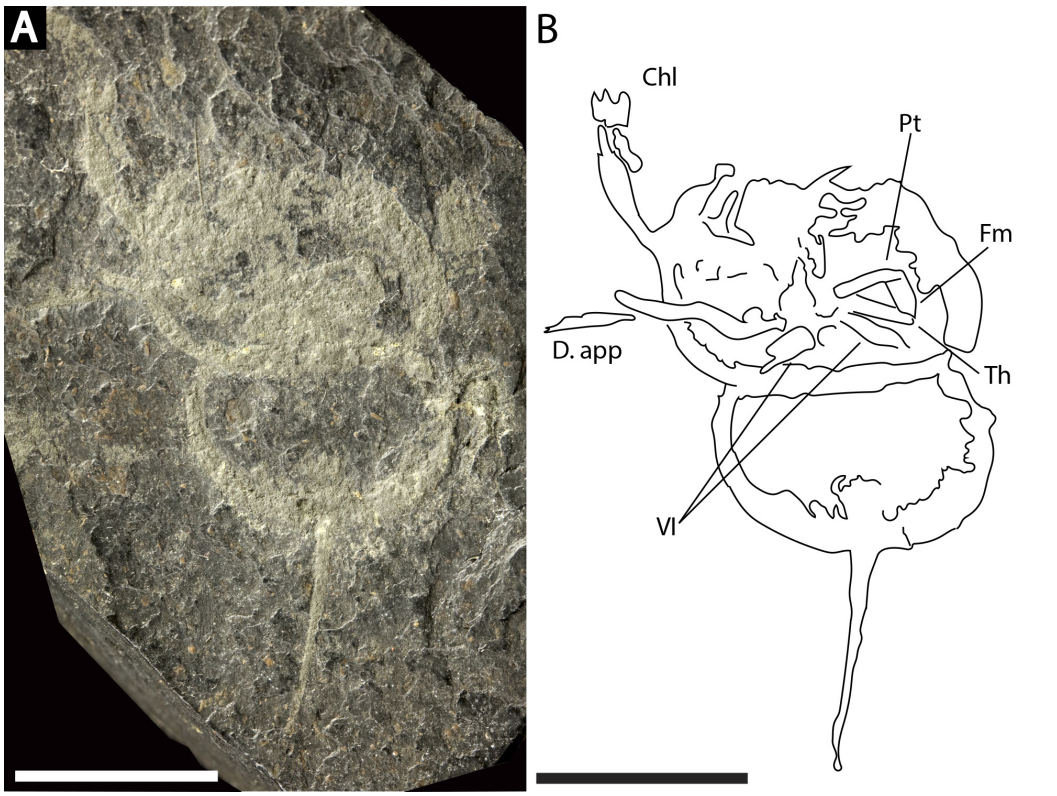

Figure 9 ***Prolimulus woodwardi*** **specimen illustrating prosomal appendage morphology.** (A) NM Me 140. (B) Interpretative drawing of specimen. Abbreviations: Chl: chelate podomeres, D.app: disarticulated appendage, VI: sixth prosomal appendage set, Pt: patella, Fm: femur, Th: trochanter. Scale bars: 10 mm. Image credit: Russell Bicknell.

Full-size DOI: 10.7717/peerj.10980/fig-9

NM M 1045 (Fig. 6): Articulated prosoma, thoracetron, and telson, preserved as a flattened impression in ventral view. Prosoma round, slightly wider than long: 11.6 mm wide and 7.5 mm long. No prosomal doublure, genal spines, lateral compound eyes, cardiac lobe, or ophthalmic ridges noted. Chelicera are only preserved appendages (Fig. 6B). Thoracetron lacks tergal expression, is round, and slightly smaller than prosoma: 10.5 mm wide and 7.5 mm long. No lateral spines noted. Thoracetron-telson articulation is a 'U'-shaped indentation in posterior thoracetron margin (Fig. 6C). Telson completely preserved, 13 mm long, and keeled. Four *Spiroglyphus vorax* specimens attached to thoracetron and all show growth lines (Fig. 6C).

NM Me 108 (Fig. 7): Twelve individuals preserved on a slab. Mean prosomal size is 11.5 mm wide and 8.4 mm long, mean thoracetron size is 10.5 mm wide and 7.4 mm long. Two individuals (F and I) are articulated. In both cases, prosomal sections rotated relative to thoracetron. Both preserve prosomal and thoracetronic doublures. No genal spines, lateral compound eyes, cardiac lobe, or ophthalmic ridges noted for either specimen. Thoracetrons lack tergal expression and lateral spines. Individual I preserved telson insertion (Fig. 7). Four individuals (C, D, E, and L) are thoracetron and telson fragments. Five individuals (A, G, H, J, and K) likely represent disarticulated prosomal sections. Individual G shows

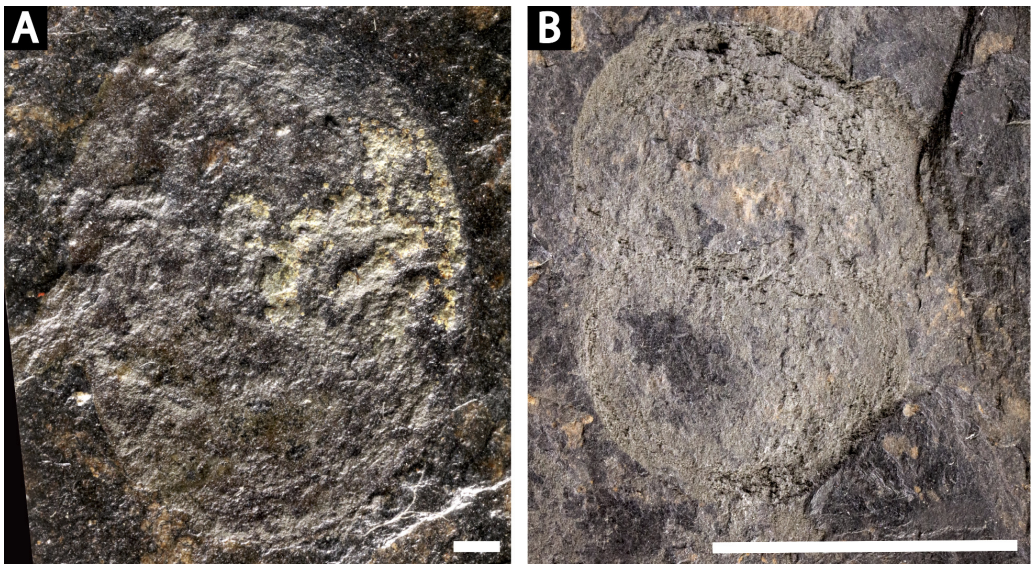

Figure 10 Poorly preserved *Prolimulus woodwardi* specimens from the National Museum of Prague Paleozoic Invertebrate collection. (A) NM Me 144. (B) NM M138. Scale bars: A: 1 mm; B: 10 mm. Image credit: Russell Bicknell.

Full-size DOI: 10.7717/peerj.10980/fig-10

a possible appendage pair on anterior prosomal edge. Individual B is fragmentary and may represent a disarticulated prosoma and thoracetron, or parts of different individuals. Cluster lacks any orientation and evidence of epibionts.

NM Me 141 (Fig. 8A): Articulated prosoma and thoracetron, poorly preserved as a flattened impression in ventral view. Prosoma round, slightly wider than long: 19.4 mm wide and 11 mm long. No prosomal doublure, genal spines, lateral compound eyes, cardiac lobe, appendages, or ophthalmic ridges noted. Only right side of thoracetron preserved. Thoracetron lacks tergal expression and lateral spines. Five *Spiroglyphus vorax* specimens attached to thoracetron.

NM Me 109 (Fig. 8B)**:** Articulated prosoma, thoracetron, and partial telson, preserved as a flattened impression in ventral view. Prosoma round, slightly wider than long: 10.3 mm wide and 5.9 mm long. No prosomal doublure, genal spines, lateral compound eyes, cardiac lobe, appendages, or ophthalmic ridges noted. Thoracetron lacks tergal expression, is round, and slightly smaller than prosoma: 9.3 mm wide and 5 mm long. No lateral spines noted. Thoracetron-telson articulation unclear, but occurs at posterior thoracetron margin. Telson partly preserved, 11 mm long. Two *Spiroglyphus vorax* specimens attached to thoracetron.

NM Me 139 (Fig. 8C)**:** Articulated prosoma, thoracetron, and partial telson, poorly preserved as a flattened impression in ventral view. Prosoma round, slightly wider than long: 20 mm wide and 15 mm long, and preserves pronounced prosomal doublure. No genal spines, lateral compound eyes, a cardiac lobe, appendages, or ophthalmic ridges noted. Thoracetron lacks tergal expression, is round, and slightly smaller than prosoma: 17 mm wide and 12 mm long. No lateral spines noted. Thoracetron-telson articulation

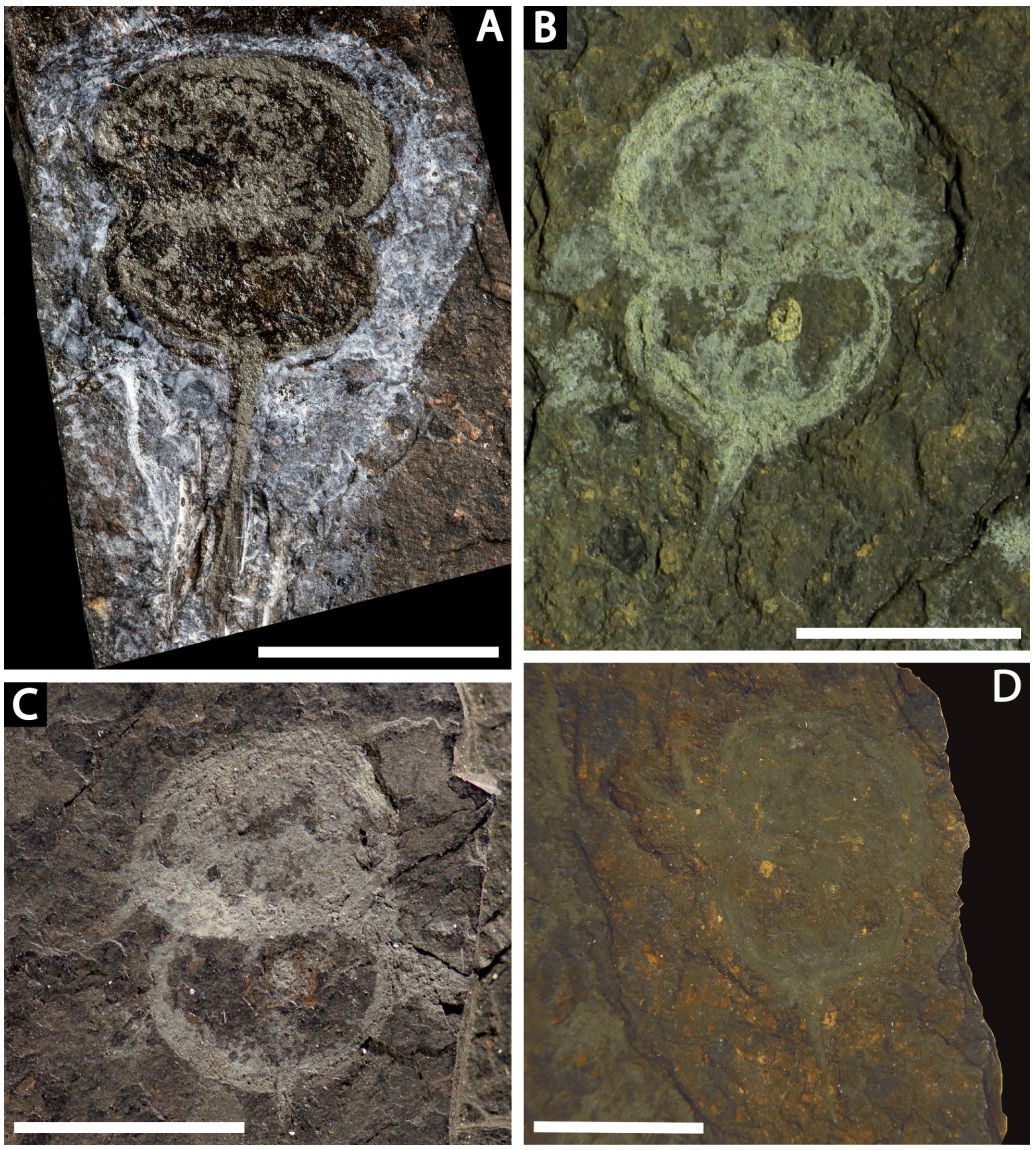

Figure 11 ***Prolimulus woodwardi*** **specimens from the Museum für Naturkunde, Leibniz-Institut, the Museum of Comparative Zoology, and the Natural History Museum.** (A) NHMUK PI In 18588; syntype. (B) NHMUK PI I 3395. (C) MCZ 109537. (D) MB.A. 1989. Scale bars: 10 mm. Image credit (A): Lucie Goodayle. (B, C): Stephen Pates. (D) Andreas Abele. Image in (A) reproduced from *Bicknell & Pates (2020)* under a CC BY 4.0 license.

Full-size DOI: 10.7717/peerj.10980/fig-11

unclear, but occurs at posterior thoracetron margin. Telson fragmentary and 4.3 mm long. Three *Spiroglyphus vorax* specimens attached to thoracetron.

NM Me 143 (Fig. 8D): Articulated prosoma and thoracetron, preserved as a flattened impression in ventral view. Prosoma round, slightly wider than long: 10 mm wide and 6.7 mm long. No prosomal doublure, genal spines, lateral compound eyes, cardiac lobe, or ophthalmic ridges noted. Thoracetron lacks tergal expression, is round, and slightly

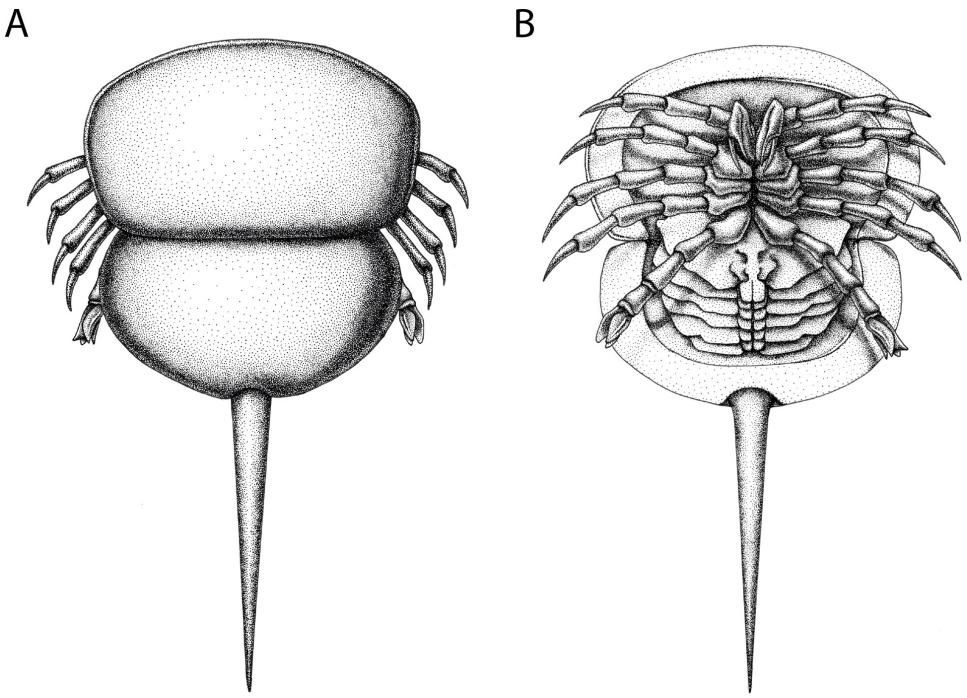

Figure 12 Reconstruction of *Prolimulus woodwardi*. (A) Dorsal anatomy based on the studied material. (B) Ventral anatomy: doublure and telson insertion based on studied material, appendages reflect details observed here and general belinurid anatomy. Reconstruction credited to Elissa Sorojsrisom.
Full-size DOI: 10.7717/peerj.10980/fig-12

smaller than prosoma: and 9.6 mm wide and 6.4 mm long. No lateral spines noted. Four *Spiroglyphus vorax* specimens attached to thoracetron (Fig. 8D).

NM Me 140 (Fig. 9): Articulated prosoma, thoracetron, and telson, preserved as a flattened impression in ventral view. Prosoma round, slightly wider than long: 14.3 mm wide and nine mm long. Prosomal doublure present. No genal spines, lateral compound eyes, cardiac lobe, or ophthalmic ridges noted. Two disarticulated prosomal appendages are preserved outside left prosomal side. Anterior appendage consists of at least a trochanter, femur, and patella, while posterior appendage possesses possible apotele and pretarsus (Fig. 9B). Two appendage sets preserved exclusively within prosomal shield. The fifth appendage on right side preserves fully articulated femoral, patellar, and trochanteral sections (Fig. 9B). Coxal sections of the sixth appendage pair also noted (Fig. 9B). Thoracetron lacks tergal expression, is round, and slightly smaller than prosoma: 11.3 mm wide and 6.5 mm long. No lateral spines noted. Thoracetron-telson articulation unclear, but occurs at posterior thoracetron margin. Telson fragmentary, 9.6 mm long.

NM Me 144 (Fig. 10A): Articulated prosoma and thoracetron, poorly preserved as a flattened impression in ventral view. Prosoma round, slightly wider than long: 8.8 mm wide and 6.5 mm long. No prosomal doublure, genal spines, lateral compound eyes, cardiac lobe, ophthalmic ridges, or appendages noted. Thoracetron lacks tergal expression, is round, and slightly smaller than prosoma: 7.7 mm wide and 7.5 mm long. No lateral spines noted.

NM Me 138 (Fig. 10B): Articulated prosoma and thoracetron, poorly preserved as a flattened impression in ventral view. Prosoma round, slightly wider than long: 10.4 mm wide and 6.9 mm long. No prosomal doublure, genal spines, lateral compound eyes, cardiac lobe, ophthalmic ridges, or appendages noted. Thoracetron lacks tergal expression, is round, and slightly smaller than prosoma: 8.8 mm wide and 6.7 mm long. No lateral spines noted.

NHMUK PI In 18588; syntype (Fig. 11A): Articulated prosoma, thoracetron and telson, preserved as a flattened impression in ventral view. Prosoma round, slightly wider than long: 14 mm wide and 7 mm long. No prosomal doublure, genal spines, lateral compound eyes, cardiac lobe, ophthalmic ridges, or appendages noted. Thoracetron lacks tergal expression, is round, and slightly smaller than prosoma: 13.2 mm wide and 6.7 mm long. No lateral spines noted. Thoracetron-telson articulation unclear, but occurs at posterior thoracetron margin. Telson fragmentary, 12.5 mm long.

NHMUK PI I 3395 (Fig. 11B): Articulated prosoma, thoracetron and telson, preserved as a flattened impression in ventral view. Prosoma round, slightly wider than long: 15.1 mm wide and 10 mm long. No prosomal doublure, genal spines, lateral compound eyes, cardiac lobe, ophthalmic ridges, or appendages noted. Thoracetron lacks tergal expression, is round, and slightly smaller than prosoma: 13.1 mm wide and eight mm long. No lateral spines are. Thoracetron-telson articulation unclear, but occurs at posterior thoracetron margin. Telson fragmentary, 9.5 mm long.

MCZ 109537 (Fig. 11C): Articulated prosoma, thoracetron and partial telson, preserved as a flattened impression in ventral view. Prosoma round, slightly wider than long: 10.8 mm wide and 8 mm long. No prosomal doublure, genal spines, lateral compound eyes, cardiac lobe, or ophthalmic ridges noted. Proximal sections of prosomal appendages are preserved outside prosoma. Thoracetron lacks tergal expression, is round, and slightly smaller than prosoma: 10 mm wide and 7 mm long. No lateral spines noted. Thoracetron-telson articulation unclear, but occurs at posterior thoracetron margin. Telson fragmentary, only articulation point preserved.

MBA. 1989 (Fig. 11D) Articulated prosoma, thoracetron and telson, preserved as a flattened impression in ventral view. Prosoma round, slightly wider than long: 13.9 mm wide and 9.9 mm long. No prosomal doublure, genal spines, lateral compound eyes, cardiac lobe, or ophthalmic ridges noted. A disarticulated appendage preserved on left side of prosoma. Thoracetron lacks tergal expression, is round, and slightly smaller than prosoma: 11.7 mm wide and 7.9 mm long. No lateral spines noted. Thoracetron-telson articulation unclear, but occurs at posterior thoracetron margin. Telson fragmentary, 6.5 mm long.

Remarks: The prosoma and thoracetron shape of *Prolimulus woodwardi* is morphologically comparable to other belinurids without genal spines (Figs. 12 and 13). However, *P. woodwardi* has a unique telson insertion morphology. In *P. woodwardi* the insertion is a 'U'-shaped indentation in the thoracetron, while *Alanops* and *Liomesaspis* lack this feature (Fig. 14). Furthermore, *Alanops* and *Liomesaspis* (Fig. 13) possess a 'thoracetronic boss', a bulge present on thoracetron over the insert of the telson. In *P. woodwardi* there is no evidence of this morphology. Finally, *Stilpnocephalus* has two notable grooves along the prosoma, not observed in *P. woodwardi*.

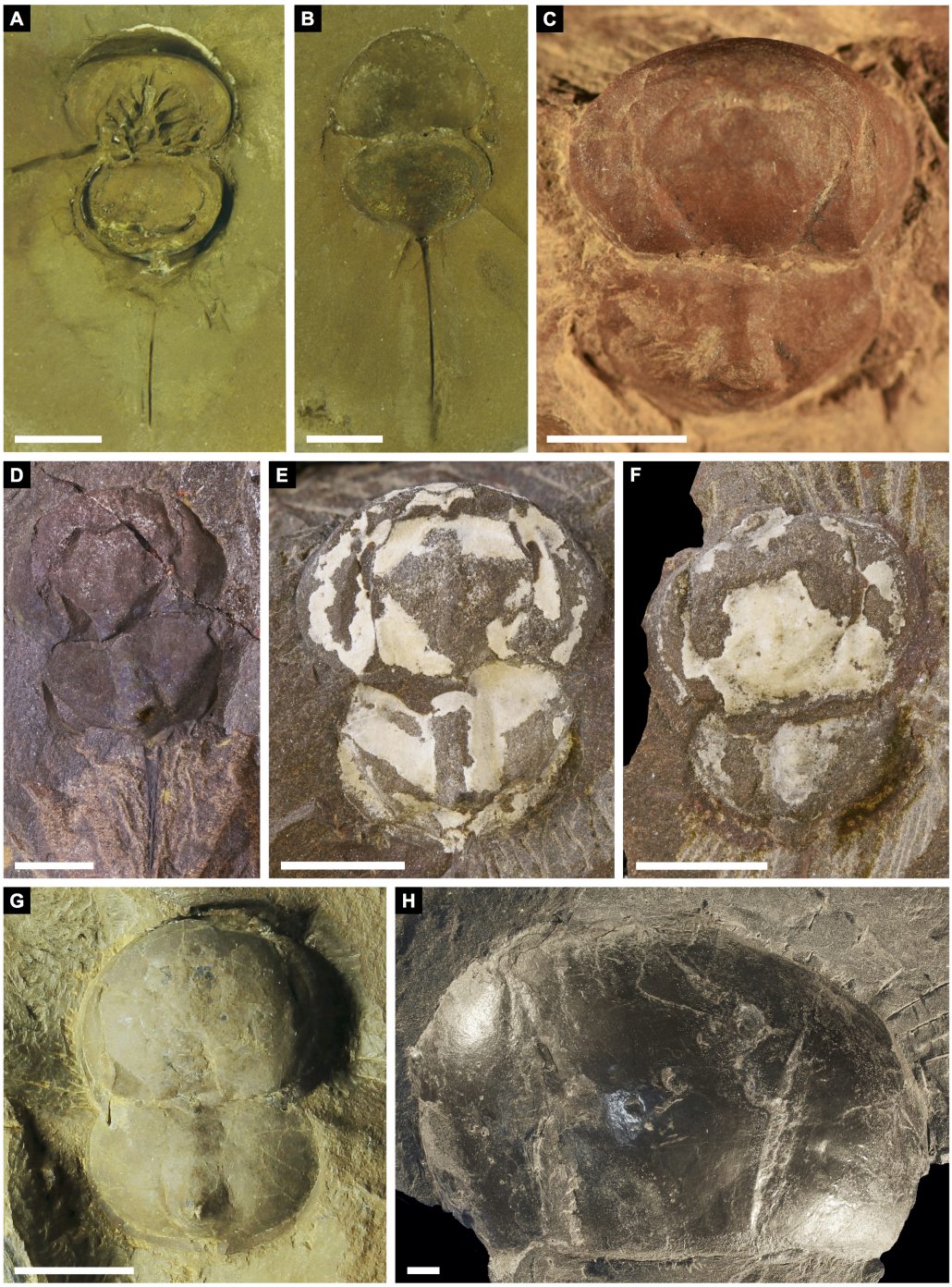

Figure 13 **Other belinurids without genal spines.** (A, B) *Alanops magnifica* from the Pennsylvanian (Stephanian)-aged Montceau-les-Mines Konservat-Lagerstätte, Great Seams Formation, France. (A) MNHN SOT001784, paratype. (B) MNHN SOT002154, paratype. (C—F) *Liomesaspis laevis* from the Pennsylvanian (Moscovian)-aged Mazon Creek *Konservat–Lagerstätte*, Carbondale Formation, USA. (C) MCZ 109536, holotype. (D) YPM IP 16913, paratype. (E) YMP IP 168041 (F) YMP IP 168053. (G) ?*Liomesaspis birtwelli* from the Pennsylvanian (Duckmantian)-aged Pennine Middle Coal Measures Formation, England, UK. NHMUK I 13882. (H) *Stilpnocephalus pontebbanus* from the Pennsylvanian (Kasimovian)-aged Meledis Formation, Friuli, MPT 18062301. Scale bars: 5 mm. Photo credit: (A, B) Dominique Chabard; (C—F) Russell Bicknell; (G) Stephen Pates; (H) Paul Selden.

Full-size DOI: 10.7717/peerj.10980/fig-13

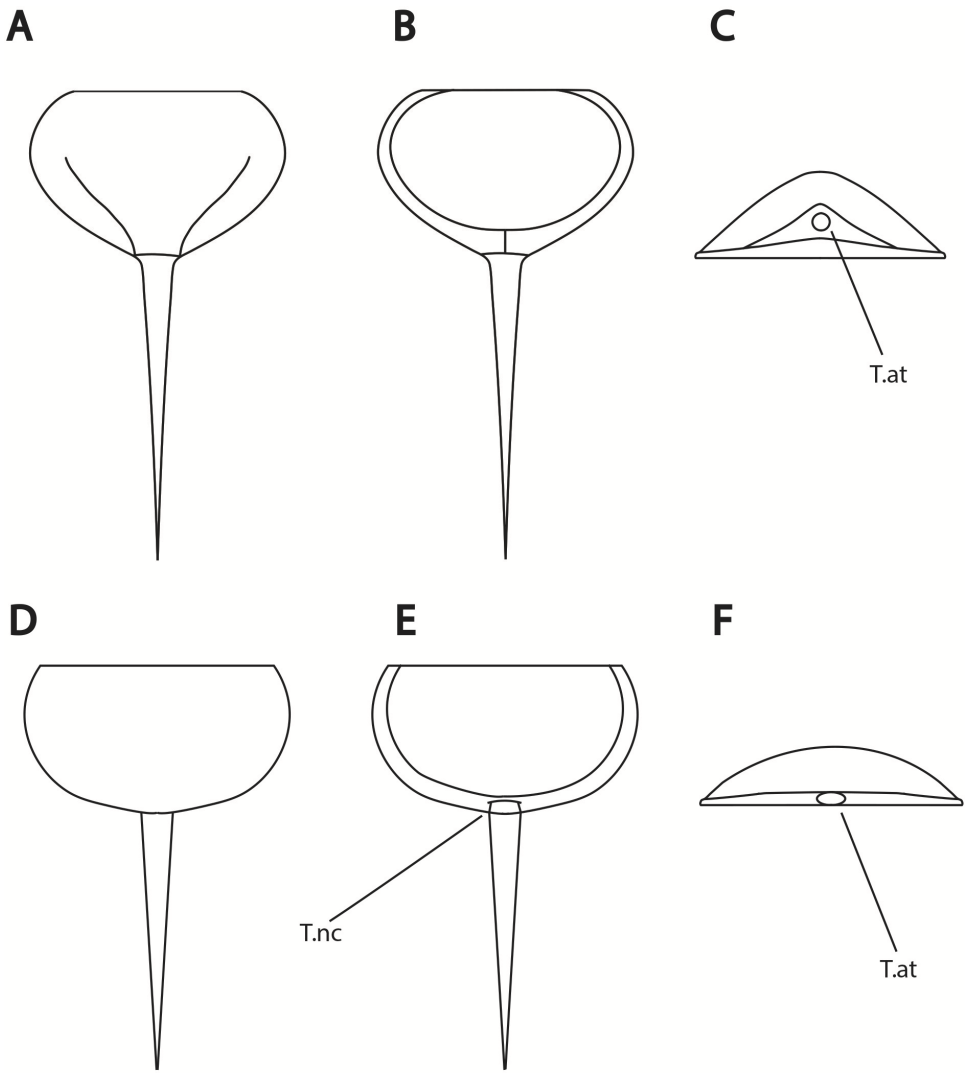

Figure 14 Differences in telson articulation between *Alanops magnificus* and *Prolimulus woodwardi*. (A–C) Schematic reconstruction of *Alanops magnificus* thoracetron and telson (modified from *Racheboeuf, Vannier & Anderson, 2002*). (A) Dorsal view. (B) Ventral view. (C) Posterior view. (D–F) Schematic reconstruction of *Prolimulus woodwardi* thoracetron and telson. (D) Dorsal view. (E) Ventral view. (F) Posterior view. Abbreviations: T.at: telson attachment, T.nc: telson notch.

Full-size DOI: 10.7717/peerj.10980/fig-14

RESULTS

Phylogenetic results

The phylogenetic analysis produced 3 trees of length 746. The strict consensus tree resultant from these trees have a comparable topology to other publications that have used the same matrix (*Lamsdell, 2016*; *Bicknell, Lustri & Brougham, 2019*; *Bicknell, Naugolnykh & Brougham, 2020*; *Bicknell & Pates, 2019*; Fig. 15). The main difference is the grouping of species within Belinurina. *Prolimulus woodwardi* resolves within a polytomy with *Liomesaspis birtwelli* (*Woodward, 1872*) and *Alanops magnificus* *Racheboeuf, Vannier &*

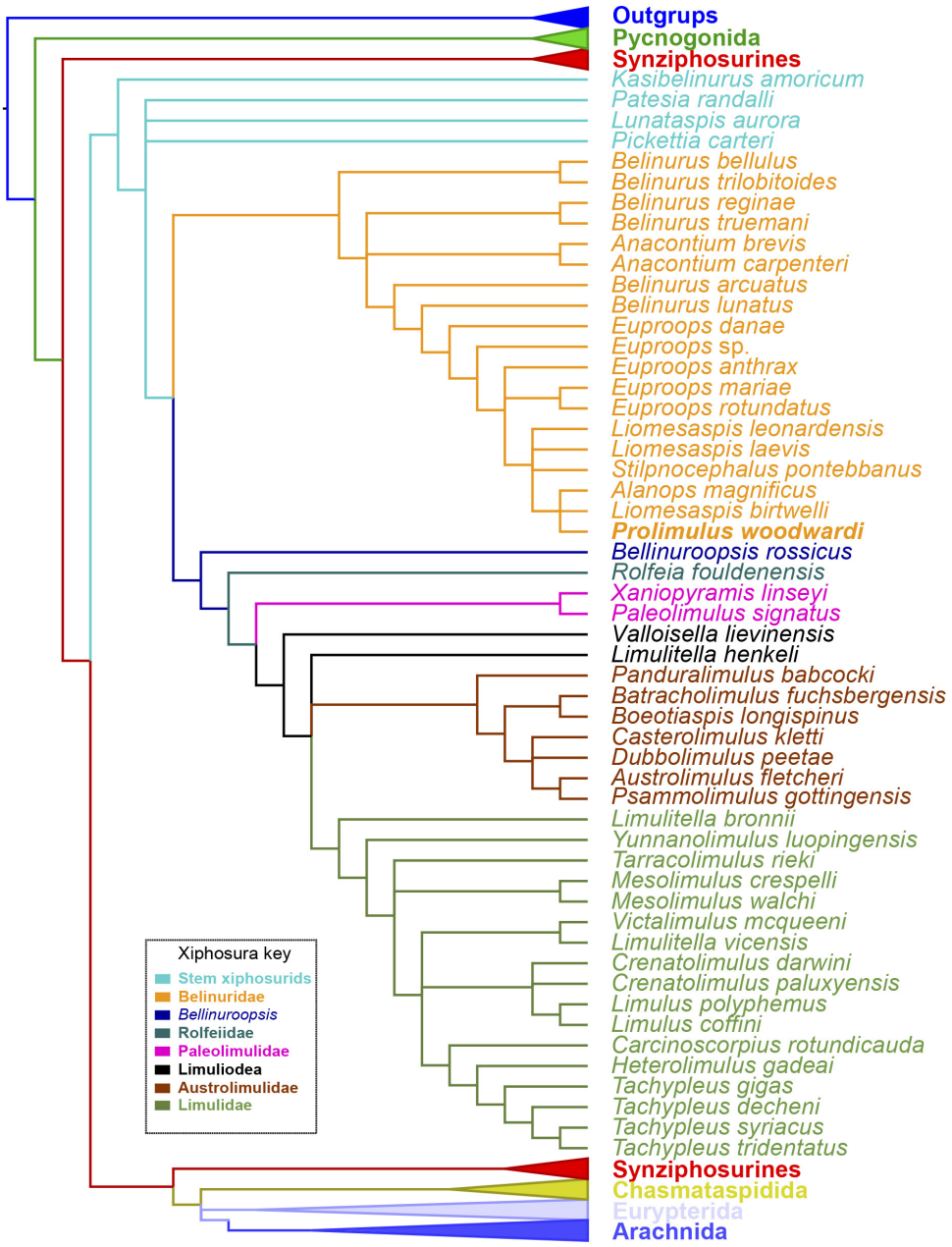

Figure 15 **Results of the phylogenetic analysis.** Strict consensus of the three trees produced by analyzing Supplementary Information 1. *Prolimulus woodwardi* is presented in bold. Topology of the outgroups, Synziphosura, Chasmataspidida, Eurypterida, and Arachnida collapsed as they are not considered here and are unchanged from other studies that used this dataset.

Full-size DOI: 10.7717/peerj.10980/fig-15

Anderson, 2002. *Stilpnocephalus pontebbanus* resolves in a polytomy containing *L. laevis* *Raymond, 1944* and *L. leonardensis* *Tasch, 1961* and the branch leading to *L. birtwelli*, *A. magnificus* and *P. woodwardi*. The autapomorphies that characterize this clade are the

reduction or absence of the genal spine, a round thoracetron with limited to no expression of tergal boundaries, and the lack of movable or fixed thoracetronic spines.

Morphometric results

The PCA plots illustrate the generic distribution of species within Belinurina in morphospace (Figs. 16 and 17). PC1 (77.7% shape variation) describes the presence or absence of the genal spine. Species within *Belinurus* and *Euproops* (sensu *Bicknell & Pates, 2020*) therefore fall into mostly positive PC1 space (Figs. 16B, 16C). By contrast, genera without genal spines—*Alanops*, *Liomesaspis*, and *Prolimulus*—dominate negative PC1 space (Fig. 16A). PC2 (9.3% shape variation) describes the posterior elongation of genal spines. This varies within *Euproops* and *Belinurus*. The specimens without genal spines are located in PC2 space of ~0, reflecting the lack of that feature. Comparing Figs. 16 and 17, the key differences are the distribution of *Belinurus*, *Koenigiella Lamsdell, 2020b* and *Prestwichianella Lamsdell, 2020b* in morphospace. *Belinurus* has a constrained distribution, while *Koenigiella* and *Prestwichianella* have extensive distributions across PC1 and PC2 respectively. Notably, *Euproops danae*—the only representative of *Euproops sensu Lamsdell (2020b)*—has the largest spread in morphospace.

DISCUSSION

Evolutionary framework of *Prolimulus* and kin

Belinurids represent the most successful Carboniferous and Permian xiphosurid group that explored freshwater niches (*Lamsdell, 2016*; *Shpinev & Vasilenko, 2018*; *Shpinev, 2018*; *Bicknell, Pates & Botton, 2019*). The group also has an exceptional diversity and disparity, which is unusual when compared to the Late Mesozoic and Cenozoic forms (*Bicknell, 2019*; *Bicknell et al., 2019a*; *Bicknell et al., in press-a*). Several attempts to colonize freshwater environments likely drove the Belinurina to evolve features that contrast the 'typical' xiphosurid morphology, and added to their extreme diversity and disparity (*Lamsdell, 2016*; *Lamsdell, 2020a*). Furthermore, freshwater environments can only sustain small populations (*Wang et al., 2019*) compared to marine conditions and are susceptible to isolating small populations (see *DeWoody & Avise, 2000*). Allopatric speciation clearly played a central role in the belinurid radiation (*Lamsdell, 2016*; *Lamsdell, 2020a*) and permitted innovative characters to be fixed within newly established populations.

The importance of heterochrony during xiphosurid evolution has recently been considered by coding such characters in a phylogenetic framework (*Lamsdell, 2020a*). This work demonstrated (among other points) that belinurid evolution generally reflects paedomorphosis. While *Lamsdell (2020a)* did not assess *Prolimulus*, paedomorphic evolution no doubt drove the development of species that are located in the same tree space in Fig. 15. The reduced body size, short or vestigial genal spines, rounded thoracetron, and absence of pre-telson epimera (terminal thoracetronic spines) are considered paedomorphic characters in Belinurina (*Lamsdell, 2020a*). The reduction or absence of genal spines and a prosoma:thoracetron ratio of ~1:1 observed in *Prolimulus*, *Alanops*, and *Liomesaspis* are also comparable to *Limulus polyphemus* (*Linnaeus, 1758*) trilobite stages

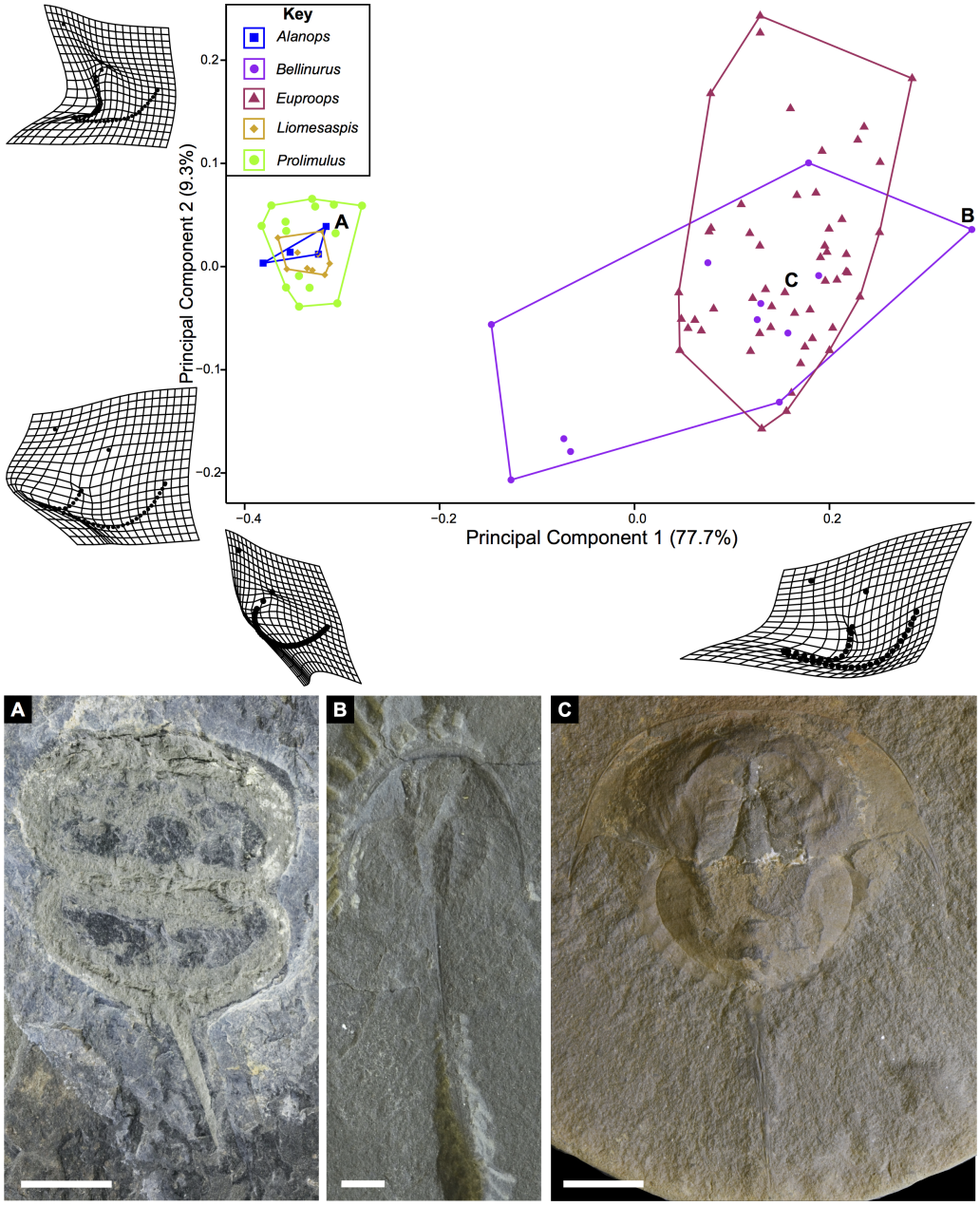

Figure 16 PCA plot of Belinurina morphospace showing PC1 and PC2 following generic assignment presented in *Bicknell & Pates (2020)*. Species with genal spines are located in PC1 space greater than −0.1. *Prolimulus woodwardi* and related species are located in more negative PC1 space. (A) *Prolimulus woodwardi* from the Pennsylvanian (Moscovian)-aged Kladno Formation. NMH L Me 142. (B) *Belinurus* c.f. *truemani Dix & Pringle, 1929* from the Pennsylvanian (Yeadonian)-aged Sprockhövel Formation, Germany. SMF.Viii.314. (C) *Euproops danae*, from the Pennsylvanian (Moscovian)-aged Mazon Creek *Konservat-Lagerstätte*, Carbondale Formation, USA. YPM IP 50659. Scale bars: 5 mm. Image credit: (A, C): Russell Bicknell. (B): Mónica Solórzano-Kraemer.

Full-size DOI: 10.7717/peerj.10980/fig-16

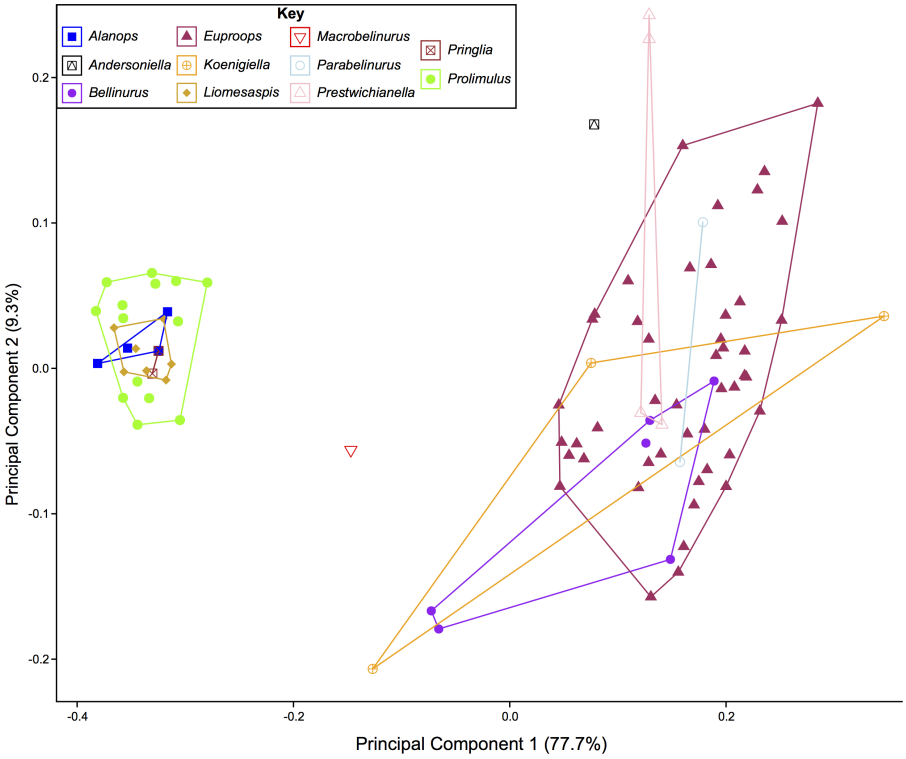

Figure 17 **PCA plot of Belinurina morphospace showing PC1 and PC2 following generic assignment presented in *Lamsdell (2020b)*.**

Full-size DOI: 10.7717/peerj.10980/fig-17

(*Fritsch, 1899*; *Prantl & Pribyl, 1955*; *Haug & Rötzer, 2018a*). However, the fossil genera display fully developed telson spines, unknown to early postembryonic *L. polyphemus* stages (*Haug & Rötzer, 2018a*). As such, the lack of genal spines and prosoma:thoracetron ratio are likely phylogenetically significant anatomical similarities, and not aspects of ontogeny. This hypothesis is supported by the *Racheboeuf, Vannier & Anderson (2002)* dataset that illustrated that the main ontogenetic modification in *A. magnificus* is increased size. The presence of juvenile characters in adult individuals of *Prolimulus* and its kin therefore represent a heterochronic event (*Gould, 1977*; *Klingenberg, 1998*). Given this unique combination of characteristics, one might consider erecting a clade to house these notably paedomorphic species. Indeed, *Raymond (1944)* had erected Liomesaspidae to contain these forms; however, this group is not used anymore. Furthermore, given the convoluted relationships between members of Belinurina, it seems unwise to re-introduce terminology. When phylogenetic and taxonomic relationships within the Belinurina are organized, it may then be pertinent to re-erect a higher order group.

Lamsdell (*2020b*, p. 17) suggested that *Prolimulus* "strong[s] affinity to *Alanops* and *Pringlia*, and there could be an argument for synonymizing *Prolimulus* with one of these genera". We disagree with this suggestion based on our observations here. The morphology of the *Prolimulus* thoracetron-telson articulation differs from *Alanops* and *Pringlia* (here considered synonymous with *Liomesaspis*, following the more conservative *Anderson*

& Selden, 1997, and amount of overlap in morphospace; Figs. 13, 17). Furthermore, a 'thoracetronic boss' is not observed in *Prolimulus* and the telson likely inserted in the thoracetronic doublure, through a telson notch (Figs. 6, 12 and 14). Regardless, if any synonymy were valid, *Alanops* or *Liomesaspis* would be synonymized with *Prolimulus* (not *vice versa*) as the Czech material has taxonomic priority.

Ethology

Clusters of extinct arthropods in the fossil record were considered evidence of biological activities (such as gregarious behavior) or traces of digestive processes (bromalite), as opposed to taphonomic artifacts (*Speyer & Brett, 1985*; *Karim & Westrop, 2002*; *Paterson et al., 2008*; *Brett et al., 2012*; *Brett, 2015*; *Bicknell, Pates & Botton, 2019*). Specimens on the sample NM Me 108 (Fig. 7) may represent such gregarious behavior. The lacustrine nature of the sapropelic coal suggest minimal physical disturbance; the individuals were therefore likely not accumulated by currents or other physical factors. As the assemblage is monospecific and has a uniform size distribution, defensive behavior can also be excluded. Interpreting this assemblage as a bromalite is also less parsimonious as there is no evidence of digestion, nor does the cluster conform to the morphology of regurgitalites, coprolites, or cololites (*Hunt, 1992*). We therefore suggest that either a moulting or mating event best explains the cluster. Horseshoe crab clustering is well documented in extant species (*Shuster Jr, 1982*; *Brockmann, 1990*; *Brockmann, 2003*; *Brockmann, Nguyen & Potts, 2000*; *Brockmann et al., 2015*); however, exceptionally rare in the horseshoe crab fossil record. Indeed, the only evidence is one possible *Euproops danae* (*Meek & Worthen, 1865*) cluster (*Ambrose & Romano, 1972*; *Fisher, 1979*; *Bicknell, Pates & Botton, 2019*). NM Me 108 (Fig. 7) therefore illustrates that clustering was potentially more common than previously thought and was employed by multiple belinurid genera.

Epibiotic organism associated with Prolimulus

Adult extant xiphosurids often experience interactions with epibionts (*Patil & Anil, 2000*; *Shuster Jr, Botton & Keinath, 2003*), while immature individuals often lack evidence of epibiotic fauna (*Allee, 1923*; *Shuster Jr, 1957*). This difference reflects frequent moulting by younger individuals, an event that removes any communities attached to the exoskeleton (*Shuster Jr & Sekiguchi, 2003*). Conversely, moulting events decrease drastically when the animals reach the sexual maturity, such that adult horseshoe crabs may have as few as one moult per year (*Carmichael, Rutecki & Valiela, 2003*). This infrequency of moulting events allows ectocommensal organisms to colonize the dorsal exoskeleton of adult horseshoe crabs. The presence and distribution of epibionts in the fossil record could therefore be used to infer developmental stages in fossil xiphosurids. Possible parasitic interaction between *Prolimulus woodwardi* (host) and *Spiroglyphus vorax* (parasite, serpulid annelid, or microconchid *Taylor & Vinn, 2006*) has been suggested (*Prantl & Pribyl, 1955*). The abundance of *S. vorax* on the studied specimens (Figs. 4A, 4B, 4D; 6A, 6B) suggests that *P. woodwardi* individuals had reached the sexual maturity and the examined population therefore represented fully adult individuals. Such evidence adds to the growing record of potential epibiotic and parasitic relationships preserved within the fossil record (see *Conway*

Morris, 1981; *Huntley & DeBaets, 2015*; *Klompmaker & Boxshall, 2015*; *Leung, 2017*; *Zhang et al., 2020*).

Comparing morphology and phylogeny of Belinurina

Xiphosurid morphospace is dominated by extreme shapes; often hypertrophied genal spines. (*Bicknell, 2019*; *Bicknell et al., 2019b*; *Bicknell & Pates, 2019*). Here, we demonstrate this condition by examining exclusively belinurid species: the constructed morphospace is polarized by species with genal spines (e.g., *Euproops* and *Belinurus*) and those lacking the morphology (e.g., *Prolimulus*, *Alanops*). Although morphospace is impacted by taphonomic modification of fossils (*Kammerer et al., 2020*), this is not apparent within the first two PCs (*Bicknell et al., 2019b*). Furthermore, as the cuticular xiphosurid exoskeleton requires exceptional preservation conditions, these fossils are seldom subject to the tectonic strain observed in trilobites (*Cooper, 1990*; *Hughes & Jell, 1992*).

Comparing the distribution of genera *Bicknell & Pates (2020)* with *Lamsdell (2020b)* allows the taxonomic framework based on phylogenetic topology to be examined and scrutinized. The position of *Macrobelinurus* *Lamsdell, 2020b* and *Andersoniella* *Lamsdell, 2020b* specimens in morphospace separate from the other clusters strongly supports the validity of these genera. Conversely, the overlap of *Parabelinuris* *Lamsdell, 2020b* with *Belinurus* and *Euproops* suggests that *Parabelinuris* represents over-splitting of the traditional genera (sensu *Bicknell & Pates, 2020*). Finally, the large spread of *Koenigiella* and *Prestwichianella* across *Belinurus* and *Euproops* suggests that either these new genera have large morphological variation, or are congeneric with *Belinurus* and *Euproops*. This over-splitting may represent the unfortunate compartmentalization of ontogenetic stages as *Belinurus* and *Euproops* taxa are may record the same ontogenetic trajectory (*Haug & Haug, 2020*). Regardless, more specimens of all genera are required for this morphospace to be more completely understood and to test the phylogenetic hypotheses of *Lamsdell (2020b)*. Furthermore, a thorough taxonomic revision of the group is needed; a work that should illustrate the range of genera, comparable to *Bicknell et al. (in press)*. Finally, and most importantly, a novel phylogenetic matrix should be constructed in tandem with such a treatise to document independently the convoluted taxonomic record of Belinurina.

CONCLUSION

Revision of *Prolimulus woodwardi*, coupled with phylogenetic and geometric morphometric analyses of belinurids, highlighted a diverse clade within Belinurina. These species without genal spines all share highly accentuated paedomorphic characters, such as vestigial genal spines, and are representative of paedomorphic evolution. A slab of multiple *P. woodwardi* individuals demonstrates new evidence for Carboniferous horseshoe crab ecology, revealing possible gregarious behavior, and further data on the deep origin xiphosurid clustering. Taken together, the examination presented here demonstrates the morphological variation and ecological conditions that permitted successful colonization of freshwater environments by Carboniferous horseshoe crabs.

INSTITUTIONAL ABBREVIATIONS

MBA	Museum für Naturkunde, Leibniz-Institut, Berlin, Germany
MCZ	Museum of Comparative Zoology, Harvard University, Cambridge, MA, USA
MNHN	Museum National d'Histoire Naturelle of Paris, Paris, France.
MPT	Museo Archeologico e Naturalistico, Tarcento, Udine, Italy
NHMUK PI	Natural History Museum, London, UK
NM	National Museum, Paleozoic Invertebrate collection, Prague, Czech Republic
SMF	Forschungsinstitut Senckenberg, Frankfurt am Main, Germany
YPM IP	Division of Invertebrate Paleontology in the Yale Peabody Museum, New Haven, Connecticut, USA

ACKNOWLEDGEMENTS

We thank Jana Bruthansová, Jessica Cundiff, Jessica Utrup, and Andreas Abele for help with the collections. We thank Stanislav Opluštil, Jan Bureš, and František Tichávek for providing valuable information on the geology, stratigraphy and mining history. We thank Andreas Abele, Dominique Chabard, Lucie Goodayle, Mónica Solórzano-Kraemer, NHM, Paul Selden, and Stephen Pates for images of specimens. We thank Elissa Sorojsrisom for her reconstruction of *Prolimulus woodwardi.* Finally, we thank Julien Kimmig and Carolin Haug for their insightful and informative reviews that helped direct and improve the text.

ADDITIONAL INFORMATION AND DECLARATIONS

Funding

This research was supported by funding from an array of sources. Lorenzo Lustria was supported by Grant no. 205321_179084 from the Swiss National Science Foundation, awarded to A. C. Daley as Principal Investigator. Lukáš Laibl was supported by institutional support RVO 67985831 of the Institute of Geology of the Czech Academy of Sciences and by Center for Geosphere Dynamics (UNCE/SCI/006). Russell D.C. Bicknell was supported by an Australian Postgraduate Award, a University of New England Postdoctoral Research Fellowship, and a James R Welch Scholarship. The funders had no role in study design, data collection and analysis, decision to publish, or preparation of the manuscript.

Grant Disclosures

The following grant information was disclosed by the authors:
Swiss National Science Foundation: 205321_179084.
Institute of Geology of the Czech Academy of Sciences: 67985831.
Center for Geosphere Dynamics: UNCE/SCI/006.
Australian Postgraduate Award.
University of New England Postdoctoral Research Fellowship
James R Welch Scholarship.

Competing Interests

The authors declare there are no competing interests.

Author Contributions

- Lorenzo Lustri and Russell D.C. Bicknell analyzed the data, prepared figures and/or tables, authored or reviewed drafts of the paper, and approved the final draft.
- Lukáš Laibl analyzed the data, prepared figures and/or tables, authored or reviewed drafts of the paper, presented the geological and geographical information, and approved the final draft.

Data Availability

The following information was supplied regarding data availability:

Raw data are available in the Supplemental Files.

Supplemental Information

Supplemental information for this article can be found online at http://dx.doi.org/10.7717/peerj.10980#supplemental-information.

REFERENCES

Adams DC, Otárola-Castillo E. 2013. geomorph: an R package for the collection and analysis of geometric morphometric shape data. *Methods in Ecology and Evolution* **4(4)**:393–399 DOI 10.1111/2041-210X.12035.

Allee WC. 1923. Studies in marine ecology: I. The distribution of common littoral invertebrates of the Woods Hole region. *The Biological Bulletin* **44(4)**:167–191 DOI 10.2307/1536774.

Ambrose T, Romano M. 1972. New upper Carboniferous Chelicerata (Arthropoda) from Somerset, England. *Palaeontology* **15(4)**:569–578.

Anderson LI, Selden PA. 1997. Opisthosomal fusion and phylogeny of Palaeozoic Xiphosura. *Lethaia* **30(1)**:19–31.

Avise JC, Nelson WS, Sugita H. 1994. A speciational history of living fossils: molecular evolutionary patterns in horseshoe crabs. *Evolution* **48(6)**:1986–2001.

Beall BS, Labandeira CC. 1990. Macroevolutionary patterns of the Chelicerata and Tracheata. *Short Courses in Paleontology* **3**:257–284 DOI 10.1017/S2475263000001823.

Bergström J. 1975. Functional morphology and evolution of xiphosurids. *Fossils and Strata* **4**:291–305.

Bicknell RDC. 2019. Xiphosurid from the Upper Permian of Tasmania confirms Palaeozoic origin of Austrolimulidae. *Palaeontologia Electronica* **22(3)**:1–13.

Bicknell RDC, Amati L, Ortega Hernández J. 2019. New insights into the evolution of lateral compound eyes in Palaeozoic horseshoe crabs. *Zoological Journal of the Linnean Society* **187(4)**:1061–1077 DOI 10.1093/zoolinnean/zlz065.

Bicknell RDC, Błazejowski B, Wings O, Hitij T, Botton ML. Critical re-evaluation of Limulidae reveals limited *Limulus* diversity. *Papers in Palaeontology* In Press DOI 10.1002/spp1002.1352.

Bicknell RDC, Brougham T, Charbonnier S, Sautereau F, Hitij T, Campione NE. 2019a. On the appendicular anatomy of the xiphosurid *Tachypleus syriacus* and the evolution of fossil horseshoe crab appendages. *The Science of Nature* **106**(**7**):38 DOI 10.1007/s00114-019-1629-6.

Bicknell RDC, Hecker A, Heyng AM. 2021. New xiphosurid fossil demonstrates Jurassic-aged extinction of Austrolimulidae. *Geological Magazine* 1–11 DOI 10.1017/S0016756820001478.

Bicknell RDC, Lustri L, Brougham T. 2019. Revision of '*Bellinurus*' *carteri* (Chelicerata: Xiphosura) from the Late Devonian of Pennsylvania, USA. *Comptes Rendus Palevol* **18**(**8**):967–976 DOI 10.1016/j.crpv.2019.08.002.

Bicknell RDC, Naugolnykh SV, Brougham T. 2020. A reappraisal of Paleozoic horseshoe crabs from Russia and Ukraine. *The Science of Nature* **107**:46 DOI 10.1007/s00114-020-01701-1.

Bicknell RDC, Pates S. 2019. Xiphosurid from the Tournaisian (Carboniferous) of Scotland confirms deep origin of Limuloidea. *Scientific Reports* **9**(**1**):17102 DOI 10.1038/s41598-019-53442-5.

Bicknell RDC, Pates S. 2020. Pictorial atlas of fossil and extant horseshoe crabs, with focus on Xiphosurida. *Frontiers in Earth Science* **8**(**98**):60 DOI 10.3389/feart.2020.00060.

Bicknell RDC, Pates S, Botton ML. 2019. *Euproops danae* (Belinuridae) cluster confirms deep origin of gregarious behaviour in xiphosurids. *Arthropoda Selecta* **28**(**4**):549–555 DOI 10.15298/arthsel.28.4.07.

Bicknell RDC, Smith PM. *Patesia* n. gen a new Late Devonian stem xiphosurid genus. *Palaeoworld* In Press DOI 10.1016/j.palwor.2020.1009.1001.

Bicknell RDC, Žalohar J, Miklavc P, Celarc B, Križnar M, Hitij T. 2019b. A new limulid genus from the Strelovec Formation (Middle Triassic, Anisian) of northern Slovenia. *Geological Magazine* **156**(**12**):2017–2030 DOI 10.1017/S0016756819000323.

Błazejowski B. 2015. The oldest species of the genus *Limulus* from the Late Jurassic of Poland. In: Carmichael RH, Botton ML, Shin PKS, Cheung SG, eds. *Changing global perspectives on horseshoe crab biology, conservation and management*. Switzerland: Springer, 3–14.

Błazejowski B, Gieszcz P, Tyborowski D. 2016. New finds of well preserved Tithonian (Late Jurassic) fossils from the Owadów-Brzezinki Quarry, Central Poland: a review and perspectives. *Volumina Jurassica* **14**(**1**):123–132.

Branson CC. 1948. Bibliographic index of Permian invertebrates. *Geological Society America Memoir* **26**:1–1049.

Brett CE. 2015. Stratigraphy and depositional environments of the Rochester Shale in western New York. In: Chinnici P, Smith K, eds. *The Silurian experience*. 2 edition. Rochester: Primitive Worlds, 36–68.

Brett CE, Zambito IVJJ, Hunda BR, Schindler E. 2012. Mid-Paleozoic trilobite Lagerstätten: models of diagenetically enhanced obrution deposits. *Palaios* **27**(**5**):326–345 DOI 10.2110/palo.2011.p11-040r.

Brockmann HJ. 1990. Mating behavior of horseshoe crabs, *Limulus polyphemus*. *Behaviour* **114**(**1**):206–220 DOI 10.1163/156853990X00121.

Brockmann HJ. 2003. Nesting behavior, a shoreline phenomenon. In: Shuster Jr CN, Barlow RB, Brockmann HJ, eds. *The American Horseshoe crab*. Cambridge: Harvard University Press, 33–49.

Brockmann HJ, Johnson SL, Smith MD, Sasson D. 2015. Mating tactics of the American horseshoe crab (*Limulus polyphemus*). In: Carmichael RH, Botton ML, Shin PKS, Cheung SG, eds. *Global perspectives on horseshoe crab biology, conservation and management*. Switzerland: Springer International, 321–351.

Brockmann HJ, Nguyen C, Potts W. 2000. Paternity in horseshoe crabs when spawning in multiple-male groups. *Animal Behaviour* **60(6)**:837–849 DOI 10.1006/anbe.2000.1547.

Bures J, Tichavek F. 2012. Prispevek k poznani fauny a flory nyranskeho sousloji (astur) na nove lokalite Pankrac u Nyran. *Zpravy o Geologickych Vyzkumech* **2011**:107–114.

Carmichael RH, Rutecki D, Valiela I. 2003. Abundance and population structure of the Atlantic horseshoe crab *Limulus polyphemus* in Pleasant Bay, Cape Cod. *Marine Ecology Progress Series* **246**:225–239 DOI 10.3354/meps246225.

Conway Morris S. 1981. Parasites and the fossil record. *Parasitology* **82(3)**:489–509 DOI 10.1017/S0031182000067020.

Cooper RA. 1990. Interpretation of tectonically deformed fossils. *New Zealand Journal of Geology and Geophysics* **33(2)**:321–332 DOI 10.1080/00288306.1990.10425690.

Crônier C, Courville P. 2005. New xiphosuran merostomata from the Upper Carboniferous of the Graissessac Basin (Massif Central France. *Comptes Rendus Palevol* **4(1-2)**:123–133 DOI 10.1016/j.crpv.2004.11.002.

DeWoody JA, Avise JC. 2000. Microsatellite variation in marine, freshwater and anadromous fishes compared with other animals. *Journal of Fish Biology* **56(3)**:461–473 DOI 10.1111/j.1095-8649.2000.tb00748.x.

Dix E, Pringle J. 1929. On the fossil Xiphosura from the South Wales Coalfield with a note on the myriapod *Euphoberia*. *Summary of Progress, Geological Survey of Great Britain* **1928**:90–113.

Eldredge N. 1974. Revision of the suborder Synziphosurina (Chelicerata, Merostomata), with remarks on merostome phylogeny. *American Museum Novitates* **2543**:1–41.

Eller ER. 1938. A new xiphosuran, *Euproops morani*, from the upper Devonian of Pennsylvania. *Annals of the Carnegie Museum* **27**:152–153.

Fisher DC. 1979. Evidence for subaerial activity of *Euproops danae* (Merostomata, Xiphosurida). In: Nitecki MH, ed. *Mazon Creek fossils*. New York: Elsevier 379–447.

Fisher DC. 1984. The Xiphosurida: archetypes of bradytely?. In: Eldredge N, Stanley SM, eds. *Living fossils*. New York: Springer 196–213.

Fritsch A. 1883. *Fauna der Gaskohle und der Kalksteine der Performation Böhmens:(Veröffenlicht mit Subvention der Kais. Akademie der Wissenshaften in Wien.) Von der Geologischen Gesellschaft in London mit dem Lyell-Preise ausgezeichnet*. F. Rivnáč.

Fritsch A. 1895. Vorläufiger Bericht über die Arthropoden und Mollusken der böhmischen Permformation. *Věstnik Královské české společnosti náuk, Třída mathematicko-přírodovědecká, Sitzungsberichte der Königl-Böhmischen Gesellschaft der Wissenschaften* **36**:1–4.

Fritsch A. 1899. Preliminary note on *Prolimulus Woodwardi*, Fritsch, from the Permian Gaskohle at Nyřan, Bohemia. *Geological Magazine* **6(2)**:57–59 DOI 10.1017/S0016756800141974.

Fritsch A. 1902. *Fauna der Gaskohle und der Kalksteine der Permformation Böhmens: Band 4: Arthropoda, Molusca, Supplement*. Reptilien: Selbstverlag.

Goloboff PA, Catalano SA. 2016. TNT version 1.5, including a full implementation of phylogenetic morphometrics. *Cladistics* **32(3)**:221–238 DOI 10.1111/cla.12160.

Gould SJ. 1977. *Ontogeny and phylogeny*. Cambridge: Harvard University Press.

Haug C, Haug JT. 2020. Untangling the Gordian knot—further resolving the superspecies complex of 300-million-year-old xiphosurids by reconstructing their ontogeny. *Development Genes and Evolution* **230(1)**:13–26 DOI 10.1007/s00427-020-00648-7.

Haug C, Rötzer MAIN. 2018a. The ontogeny of *Limulus polyphemus* (Xiphosura s. str. Eucheliceratа) revised: looking under the skin. *Development Genes and Evolution* **228(1)**:49–61 DOI 10.1007/s00427-018-0603-1.

Haug C, Rötzer MAIN. 2018b. The ontogeny of the 300 million year old xiphosuran *Euproops danae* (Eucheliceratа) and implications for resolving the *Euproops* species complex. *Development Genes and Evolution* **228(1)**:63–74 DOI 10.1007/s00427-018-0604-0.

Haug C, Van Roy P, Leipner A, Funch P, Rudkin DM, Schöllmann L, Haug JT. 2012. A holomorph approach to xiphosuran evolution—a case study on the ontogeny of *Euproops*. *Development Genes and Evolution* **222(5)**:253–268 DOI 10.1007/s00427-012-0407-7.

Hughes NC, Jell PA. 1992. A statistical/computer-graphic technique for assessing variation in tectonically deformed fossils and its application to Cambrian trilobites from Kashmir. *Lethaia* **25(3)**:317–330 DOI 10.1111/j.1502-3931.1992.tb01401.x.

Hunt AP. 1992. Late Pennsylvanian coprolites from the Kinney Brick Quarry, central New Mexico, with notes on the classification and utility of coprolites. *New Mexico Bureau of Mines and Mineral Resources, Bulletin* **138**:221–229.

Huntley JW, De Baets K. 2015. Trace fossil evidence of trematode—bivalve parasite—host interactions in deep time. *Advances in parasitology* **90**:201–231.

Kammerer CF, Deutsch M, Lungmus JK, Angielczyk KD. 2020. Effects of taphonomic deformation on geometric morphometric analysis of fossils: a study using the dicynodont *Diictodon feliceps* (Therapsida, Anomodontia). *PeerJ* **8**:e9925 DOI 10.7717/peerj.9925.

Karim T, Westrop SR. 2002. Taphonomy and paleoecology of Ordovician trilobite clusters, Bromide Formation, south-central Oklahoma. *Palaios* **17(4)**:394–402 DOI 10.1669/0883-1351(2002)017<0394:TAPOOT>2.0.CO;2.

Kin A, Błażejowski B. 2014. The horseshoe crab of the genus *Limulus*: living fossil or stabilomorph? *PLOS ONE* **9(10)**:e108036 DOI 10.1371/journal.pone.0108036.

Klingenberg CP. 1998. Heterochrony and allometry: the analysis of evolutionary change in ontogeny. *Biological Reviews* **73(1)**:79–123.

Klompmaker AA, Boxshall GA. 2015. Fossil crustaceans as parasites and hosts. *Advances in parasitology* **90**:233–289.

Krawczyński W, Filipiak P, Gwoździewicz M. 1997. Zespółskamieniałości z karbońskich sferosyderytów (westfal A) NE części Górnośląskiego Zagłębia Węglowego. *Przeglad Geologiczny* **45(12)**:1271–1274.

Krs M, Krsová M, Pruner P. 1995. Palaeomagnetism and palaeogeography of Variscan formations of the Bohemian Massif: a comparison with other regions in Europe. *Studia Geophysica et Geodaetica* **39(3)**:309–319 DOI 10.1007/BF02295824.

Lamsdell JC. 2013. Revised systematics of Palaeozoic 'horseshoe crabs' and the myth of monophyletic Xiphosura. *Zoological Journal of the Linnean Society* **167(1)**:1–27 DOI 10.1111/j.1096-3642.2012.00874.x.

Lamsdell JC. 2016. Horseshoe crab phylogeny and independent colonizations of fresh water: ecological invasion as a driver for morphological innovation. *Palaeontology* **59(2)**:181–194 DOI 10.1111/pala.12220.

Lamsdell JC. 2020a. A new method for quantifying heterochrony in evolutionary lineages. *Paleobiology* Epub ahead of print 2020 13 May DOI 10.1017/pab.2020.17.

Lamsdell JC. 2020b. The phylogeny and systematics of Xiphosura. *PeerJ* **8**:e10431 DOI 10.7717/peerj.10431.

Lamsdell JC, McKenzie SC. 2015. *Tachypleus syriacus* (Woodward)—a sexually dimorphic Cretaceous crown limulid reveals underestimated horseshoe crab divergence times. *Organisms Diversity & Evolution* **15(4)**:681–693 DOI 10.1007/s13127-015-0229-3.

Latreille PA. 1802. *Histoire naturelle générale et particulière des crustacés et des insectes: ouvrage faisant suite aux owuvres de Leclerc de Buffon, et partie du cours complet d'histoire naturelle rédigé par CS Sonnini, membre de plusieurs Sociétés savantes.* Paris: Dufart.

Leung TL. 2017. Fossils of parasites: what can the fossil record tell us about the evolution of parasitism? *Biological Reviews* **92(1)**:410–430 DOI 10.1111/brv.12238.

Linnaeus C. 1758. *Systema naturæper regna tria naturæ, secundum classes, ordines, genera, species, cum characteribus, differentiis, synonymis, locis.* Holmia: Laurentius Salvius.

Meek FB, Worthen AH. 1865. Notice of some new types of organic remains, from the Coal Measures of Illinois. *Proceedings of the Academy of Natural Sciences of Philadelphia* **17(1)**:41–48.

Opluštil S, Martínek K, Tasáryová Z. 2005. Facies and architectural analysis of fluvial deposits of the Nýřany Member and the Týnec Formation (Westphalian D–Barruelian) in the Kladno-Rakovník and Pilsen basins. *Bulletin of Geosciences* **80(1)**:45–66.

Opluštil S, Schmitz M, Cleal CJ, Martínek K. 2016. A review of the Middle–Late Pennsylvanian west European regional substages and floral biozones, and their

correlation to the Geological Time Scale based on new U–Pb ages. *Earth-Science Reviews* **154**:301–335 DOI 10.1016/j.earscirev.2016.01.004.

Opluštil S, Šimůnek Z, Zajíc J, Mencl V. 2013. Climatic and biotic changes around the Carboniferous/Permian boundary recorded in the continental basins of the Czech Republic. *International Journal of Coal Geology* **119**:114–151 DOI 10.1016/j.coal.2013.07.014.

Paterson JR, Hughes NC, Chatterton BD, Rábano I. 2008. Trilobite clusters: what do they tell us? A preliminary investigation. *Advances in Trilobite Research* **9**:313–318.

Patil JS, Anil AC. 2000. Epibiotic community of the horseshoe crab *Tachypleus gigas*. *Marine Biology* **136(4)**:699–713 DOI 10.1007/s002270050730.

Pešek J. 1994. *Carboniferous of central and western Bohemia (Czech Republic): Czech geol.* Survey Prague.

Pešek J, Sivek M, Sivek M. 2016. *Coal-bearing basins and coal deposits of the Czech Republic*. Prague: Czech Geological Survey.

Pictet F-J. 1846. *Traité élémentaire de paléontologie ou histoire naturelle des animaux fossiles*. Paris: Baillière.

Prantl F, Pribyl A. 1955. Ostrorepi (Xiphosura) ceskoslovenskeho karbonu. *Sborník Ústředního Ústavu Geologického* **23**:379–424.

Purkyně C. 1899. Nýřanská sloj uhelná u Nýřan. *Rozpravy České akademie císaře Františka Josefa pro vědy, slovesnost a umění - Třída 2* **8(31)**:1–30.

Racheboeuf PR, Vannier J, Anderson LI. 2002. A new three-dimensionally preserved xiphosuran chelicerate from the Montceau-les-Mines Lagerstätte (Carboniferous, France). *Palaeontology* **45(1)**:125–147 DOI 10.1111/1475-4983.00230.

Raymond PE. 1944. Late Paleozoic xiphosurans. *Bulletin of the Museum of Comparative Zoology* **94**:475–508.

Rosa CLM, Grangeiro ME, Bocalon VLS, Netto RG. 1994. Craticulichnum iruiensis: Uma nova contribuição à paleoicnologia da seqüência sedimentar Rio Bonito/-Palermo no RS1. *Acta Geologlca Leopoldensla* **17(39)**:33–45.

Rudkin DM, Young GA. 2009. Horseshoe crabs–an ancient ancestry revealed. In: Tanacredi JT, Botton ML, Smith DR, eds. *Biology and conservation of horseshoe crabs*. New York: Springer, 25–44.

Shuster Jr CN, Botton ML, Keinath JA. 2003. Horseshoe crabs in a food web: who eats whom. In: Shuster Jr CN, Barlow RB, Brockmann HJ, eds. *The American horseshoe crab*. Cambridge: Harvard University Press, 133–153.

Selden PA, Simonetto L, Marsiglio G. 2019. An effaced horseshoe crab (Arthropoda: Chelicerata: Xiphosura) from the Upper Carboniferous of the Carnic Alps (Friuli, NE Italy). *Rivista Italiana di Paleontologia e Stratigrafia* **125(2)**:333–342.

Selden PA, Siveter DJ. 1987. The origin of the limuloids. *Lethaia* **20(4)**:383–392 DOI 10.1111/j.1502-3931.1987.tb00800.x.

Shpinev ES. 2018. New data on Carboniferous xiphosurans (Xiphosura, Chelicerata) of the Donets Coal Basin. *Paleontological Journal* **52(3)**:271–283 DOI 10.1134/S0031030118030127.

Shpinev E, Vasilenko D. 2018. First fossil xiphosuran (Chelicerata, Xiphosura) egg clutch from the Carboniferous of Khakassia. *Paleontological Journal* **52(4)**:400–404 DOI 10.1134/S0031030118040111.

Shuster Jr CN. 1982. A pictorial review of the natural history and ecology of the horseshoe crab *Limulus polyphemus*, with reference to other Limulidae. *Progress in Clinical and Biological Research* **81**:1–52.

Shuster Jr CN. 1957. Xiphosura (with especial reference to *Limulus polyphemus*). *Geological Society of America Memoirs* **67**:1171–1174.

Shuster Jr CN, Sekiguchi K. 2003. Growing up takes about ten years and eighteen stages. In: Shuster Jr CN, Barlow RB, Brockmann HJ, eds. *The American horseshoe crab*. Cambridge: Harvard University Press 103–132.

Speyer SE, Brett CE. 1985. Clustered trilobite assemblages in the Middle Devonian Hamilton group. *Lethaia* **18(2)**:85–103 DOI 10.1111/j.1502-3931.1985.tb00688.x.

Størmer L. 1952. Phylogeny and taxonomy of fossil horseshoe crabs. *Journal of Paleontology* **63**:0–640.

Strauch F. 1966. Zur Autökologie und über bemerkenswerte Funde von *Spirorbis* Daudin 1800 (Polychaeta sedentaria) im Oberkarbon des Saargebietes. *Paläontologische Zeitschrift* **40(3–4)**:269–273 DOI 10.1007/BF02988178.

Štamberg S, Zajíc J. 2008. *Carboniferous and Permian faunas and their occurence in the limnic basins of the Czech Republic*. Museum of Eastern Bohemia.

Tasch P. 1961. Paleolimnology: Part 2: Harvey and Sedgwick Counties, Kansas: Stratigraphy and Biota. *Journal of Paleontology* **35(4)**:836–865.

Taylor PD, Vinn O. 2006. Convergent morphology in small spiral worm tubes ('Spirorbis') and its palaeoenvironmental implications. *Journal of the Geological Society* **163(2)**:225–228 DOI 10.1144/0016-764905-145.

VanRoy P, Briggs DEG, Gaines RR. 2015. The Fezouata fossils of Morocco; an extraordinary record of marine life in the Early Ordovician. *Journal of the Geological Society* **172(5)**:541–549 DOI 10.1144/jgs2015-017.

Wang T, Fujiwara M, Gao X, Liu H. 2019. Minimum viable population size and population growth rate of freshwater fishes and their relationships with life history traits. *Scientific Reports* **9(1)**:1–8 DOI 10.1038/s41598-018-37186-2.

Weygoldt P, Paulus HF. 1979. Untersuchungen zur Morphologie, Taxonomie und Phylogenie der Chelicerata 1 II. Cladogramme und die Entfaltung der Chelicerata. *Journal of Zoological Systematics and Evolutionary Research* **17(3)**:177–200.

Woodward H. 1872. Notes on some British Palæozoic Crustacea belonging to the order Merostomata. *Geological Magazine* **9(100)**:433–441 DOI 10.1017/S0016756800465386.

Zhang Z, Strotz LC, Topper TP, Chen F, Chen Y, Liang Y, Zhang Z, Skovsted CB, Brock GA. 2020. An encrusting kleptoparasite-host interaction from the early Cambrian. *Nature Communications* **11(1)**:1–7 DOI 10.1038/s41467-019-13993-7.

Zittel KAv, Eastman CR. 1913. *Textbook of Palaeontology*. London: Macmillan.